Evaluation and Implementation of a Dosimetry Protocol for Lutetium Lu 177 DOTATATE for the Treatment of Gastroenteropancreatic-Neuroendocrine Tumors

by

Jared Stoller

A thesis

Presented to the Medical Physics Graduate Program

and the Oregon Health and Science University

School of Medicine

in partial fulfillment of

the requirements for the degree of

Master of Science

June 2nd, 2022

Contents

List of Figures

List of Tables

1 Acknowledgements

I would like to first acknowledge and thank my professors, mentors, and advisors for this project, Dr. Mittra, Dr. Mench, Dr. Pugachev, and Dr. Graves. All of whom guided throughout this entire project and gave me the tools necessary to make this possible.

I would next like to acknowledge and thank all of my mentors throughout my education. Though there are too many to name, all have made an incredible impact on the person that I am today. Their time as teachers, professors, coaches, and friends have inspired me to try to emulate their ability to reach others in a meaningful way.

I would next like to thank my parents. My mom and dad have given me so much love and support my entire life. I am not exaggerating when I say that I would not have made it here without them. They have kept me grounded and nurtured. Words cannot possibly describe how thankful I am for that.

Lastly, I would like to thank my partner Rebecca. I am eternally thankful that she moved all the way across the country to be with me. She is my other half and I feel complete with her with me. She is with me at my highs and at my lows, always supporting me in every way she can.

2 Abstract

Introduction

Lutathera is a radiopharmaceutical used to treat gastroenteropancreatic-neuroendocrine tumors(GEP-NETs) in adults that are positive for hormone receptor somatostatin. The current FDA-approved label describes Lutathera treatment as four 200 mCi cycles given every eight weeks. If the patient reacted negatively to toxicity caused by acute myelosuppression which is a decrease in bone marrow activity which leads to fewer red blood cells, white blood cells, and platelets, or nephrotoxicity(1), the dose is halved to 100 mCi. If the patient continues to experience toxicity from the radiopharmaceutical, the treatment is stopped. A dosimetry protocol will outline the imaging modality utilized to obtain quantitative information about the distribution of Lutathera, the frequency at which imaging needs to occur, and the time after injection that imaging needs to occur. Personalized dosimetry would also allow for an increase of prescribed activity with the gain in knowledge of the proximity to dose thresholds leading to deterministic effects for organs at risk.

Methods

An imaging protocol for Lutathera was designed based on a literature review of several clinics' proprietary protocols. The three main protocols that have been evaluated are intended to match the needs and capabilities of the OHSU Nuclear Medicine and Molecular Imaging Clinic. One is a more intensive, four time point protocol. This protocol includes a SPECT/CT scan on the day of treatment to establish a baseline, one SPECT/CT scan twenty-four hours post injecting, one SPECT/CT scan at day four after injection, and a late time-point at either day five or eight after injection. Contoured SPECT/CT images will be imported into MIM where integrated activity will be used to created TACs, calculate TIACs, generated Dose-Volume Histograms, and cumulative dose to each organ and lesion in Sureplan MRT and OLINDA.

Results

The doses to organs at risk and tumors were evaluated in both MIM© and OLINDA©. The capabilities and outputs of both software programs vary and the data presented reflects that. MIM SurePlan MRT Lutathera package is able to create dose maps, Dose Volume Histograms, and Time-Activity curves. OLINDA 1.0 is only capable of producing dose per activity rates for each organ with the additional capability of scaling the calculation based on organ volume. The additional calculations for OLINDA were completed in Excel© including the calculation of time-integrated activity curves and dose to organs at risk. The data provided by both softwares showed the importance of the baseline and 96 hour time point scans as higher deviation from the standard dose were seen without the baseline scan in the three time point protocol. Therefore, although the four time-point method has the highest accuracy, the three and two-point methods offer a good balance between accuracy and practicality.

Conclusion

The dosimetry protocol used by a clinic has to consider logistical factors as well as protocol accuracy. A four-time point protocol after each cycle of Lutathera provides the greatest amount of data to calculate the dose to organs at risk as well as lesions but is also the most laborious for dosimetrists and burdening towards patients. In order to be able to handle the workload for more patients as well as have patients agree to extra scans, three and single time point protocols also provide a viable option toward patient-specific dosimetry. In the case where patients do not wish to receive three extra SPECT/CT scans or clinic layout prohibits day zero imaging, single and three time point imaging protocols, respectively, can be used, however the single time point protocol offers less deviation from the four time point protocol than the three time point protocol.

3 Introduction and Aim of Study

The goal of this project is to establish a dosimetry protocol for lutetium Lu-177 DOTATATE (Lutathera). A dosimetry protocol will outline the imaging modality utilized to obtain quantitative information about the distribution of Lutathera, the frequency at which imaging needs to occur, and the time after injection that imaging needs to occur. The modality, frequency, and timing of imaging will match the uptake and decay parameters of Lutathera to gain adequate quantitative information for dosimetry. The protocol will consist of two, three, or four SPECT/CT scans to gather date on activity in organs of interest will. Further decisions leading to the formulation of the Lutathera Dosimetry Protocol will be evaluated in both aims of this project.

The length and rigor of the protocol will be evaluated through aim one of this project. The first aim of this project will assess the statistical difference between the dose calculated from a four time point protocol, that can last between five and eight days post treatment, compared to a shorter four day protocol consisting of two time points, and a three time point protocol that omits the baseline scan and better fits the logistics of OHSU's clinic.

The second aim of this project is going to asses the doses calculated to organs at risk using two different dosimetric softwares, Organ Level Internal Dosimetry Assessment(OLINDA)© and MIM©. Both softwares have the capability of determining dose from SPECT/CT data but utilize different methods in achieving this task. OLINDA uses a stylized phantom to calculate dose and MIM uses voxelized dosimetry to accomplish the same task. The capabilities and features of both softwares will be explained in greater detail in the background.

Lutathera is a radiopharmaceutical used to treat gastroenteropancreatic-neuroendocrine tumors(GEP-NETs) in adults that are positive for hormone receptor somatostatin. Lutetium-177, which serves as the radionuclide in this drug, is a beta-emitter (83.47%). Beta particles have a relatively short range and low linear energy transfer(LET) which is why this decay method is used in nuclear medicine therapies. One of the main classifications of low grade neuroendocrine tumors is the over-expression of the somatostatin(SSTR) receptor 2.(2) So-

matostatin is a hormone that helps regulate the endocrine system. The pharmaceutical component of Lutathera, DOTATATE is a peptide that is analogous to somatostatin in regard to it's affinity to SSTR2 but not in biochemical behavior. This means that when injected into the body, DOTATATE will preferentially migrate to SSTR2 but will not follow the biochemical pathway of somatostatin. Since neuroendocrine tumors over-express SSTR2, DOTATATE will guide the radiopharmaceutical towards neuroendocrine tumors.

The current FDA-approved label describes Lutathera treatment as four 200 mCi cycles given every eight weeks. If the patient reacted negatively to toxicity caused by acute myelosuppression which is a decrease in bone marrow activity which leads to fewer red blood cells, white blood cells, and platelets, or nephrotoxicity(1), the dose is halved to 100 mCi. If the patient continues to experience toxicity from the radiopharmaceutical, the treatment is stopped. The major organs at risk of deterministic effects from radiation are the kidneys, spleen, liver, and bone marrow. Toxicity to the kidneys, liver, and primarily the bone marrow serve as a limiting factor to this treatment as the adverse effects from toxicity to any of these regions can be life-threatening. The motivation for this project is to create a dosimetry protocol for this treatment in order to gain more information about the true distribution of the Lutathera to not only the tumors themselves but to organs at risk as well.

A dosimetry protocol can be utilized to provide personalized dosimetry for this treatment in order to gain more information about the true distribution of Lutathera to not only the tumors themselves but to organs at risk as well. This would prevent discrete reductions in prescription and could allow for treatment to continue with a mathematically determined prescription adjustment. Personalized dosimetry would also allow for an increase of prescribed activity with the gain in knowledge of the proximity to dose thresholds leading to deterministic effects for organs at risk.

Kidney function and drug distribution vary from person to person and therefore it may can be inferred that a standard FDA-approved label of four, 200 mCi cycles given approximately every eight weeks may not yield the same results in every patient. Some patients

may be able to handle another cycle or a higher dose while others may experience toxicity. When implemented, this dosimetry protocol may determine the group each patient falls under, which in the future could allow for a precision medicine approach for each patient as the dose can be modulated to ensure the lowest amount of radiation induced toxicity and highest lesional dose and therefore allows for personalized dosimetry. This would mean that patients receiving Lutathera treatment can be given an injected activity specific to the rate of clearance in their body as well as the effectiveness of radiopharmaceutical uptake in NETs. Knowing the dose to lesions as well as organs at risk is a significant feature of nuclear medicine dosimetry and can lead to more effective treatments.

With other radiopharmaceuticals like Iobenguane I-131(Azedra or MIBG), there is a standardized method to conduct personalized dosimetry. Part of the initial planning involved making a spreadsheet to visualize the similarities in planning from clinic to clinic. From there we have worked to tailor each approach to fit our department. Due to logistical issues of having Lutathera treatment occur on the Marquam Hill campus and with only research grade SPECT/CTs located on the waterfront campus, the early imaging time point of around four hours became a near impossibility for the current setup at OHSU.

The literature review alone did not lead to a preferred method of how to best design OHSU's dosimetry protocol for Lutathera. Each hospital made proprietary decisions as to how many time points to use, whether to image with Whole Body Planar,SPECT/CT, or a combination of both, and what dosimetry software to utilize(3). The methods that this project are evaluating follow four time points, similar to University of Montpellier(4), three time points, similar to Uppsala University(5), and a two time point which includes a baseline scan, similar to University of Iowa(6). It should be noted that for the University of Iowa's protocol, only one time point is used and pharmacokinetic information is assumed to complete the dose calculation. This project will instead use the information from the baseline scan and another time point to evaluate this protocol. The 96-hour time point, imaged in both Deep Blue Data patients, is particularly highlighted as the time point between where

the kidneys and liver are best imaged for dosimetric purposes(7). There is additional detail as to the specific times selected by each group but variation from the Deep Blue Repository data was not feasible for this project. Additionally, the MIRD 26 Pamphlet outlines in detail how to build a comprehensive dosimetry protocol for Lu-177 dosimetry(8)(9).

To determine if this logistical issue was going to be detrimental to the goal by resulting in a less accurate imaging model, this project is evaluating three protocols with the same data sets, provided by the University of Michigan(10), to find the percentage dose difference between each protocol. This project was created as a sub-project/result of the overarching idea of personalized dosimetry for Lutathera at OHSU. The answer required an evaluation of the department layout and individual protocol efficiency. The three protocols being evaluated, four time points, three time points, and two time points, represent different degrees of convenience and feasibility. The goal is to compare each protocol based not only on convenience and feasibility but also accuracy and reliability of the dose calculation.

Each dosimetry protocol will consist of 2-4 scans in the first week after the first cycle of treatment. The first of the protocols will include four time points in which patients will undergo a SPECT/CT scan at 4 hours, 24 hours, 96 hours, and 124/192 hours. This will represent the most rigorous of the three protocols but also the most time consuming one. The doses calculated for the other two protocols will be compared to this protocol. The reason that the four time point protocol will serve as the standard for the other two protocols is that it provides the most amount of data points, but also follows the uptake and clearance patterns of Lutathera. After injection, Lutathera begins to be taken up by lesions and organs at risk. This process ends about twenty-four hours post treatment. After this uptake period, clearance begins to take place and the activity in lesions and organs begins to decrease. The four time point protocol images during the uptake, at the approximate apex of activity, and at later time points were clearance is taking place. The second protocol that will be evaluated will be the three time point protocol. This is the predictably intermediate protocol that would be the most feasible for OHSU at this time as it excludes the four hour

time point that will not be able to take place until the treatment area is in the same location as a research grade SPECT/CT. Aim one will seek to determine if missing the quantitative data of radiopharmaceutical uptake will result in a highly deviated dose calculation or if this first scan is imperative. The last of the three protocols is referred to as the two time point protocol. The first being the four hour time point and the latter being the third time point that is around the 96 hour mark. The 96 hour time point was chosen as it yields that best results when calculating dose to the kidneys, tumor, and liver(6)(11). The calculation method used utilizes the least squares method to fit an exponential curve to the Time-Activity curve. This method requires at least two points to create a viable exponential curve to approximate the activity of the radiopharmaceutical left in a region of the body at a given time. The single time point method is the quickest and least cumbersome of the three protocols for the patients and staff involved in treatment and dosimetry as it requires the least amount of follow up post treatment. It also images one time point during uptake and one time point during clearance. This protocol provides the least amount of data points to create an exponential fit, requiring the rate constant parameter to be held constant(representing population average), and therefore has the potential to not be as accurate.

The count data will be manually transferred from MIM into Excel and MIM's SurePlan MRT software which determines counts per voxel from the scan data. Count per voxel can be used to estimate the dose in each region of interest in the body. The 2-4 scans over the first week will provide multiple time points that will be used to create time-activity curves, showing the amount of activity present in the body at a given time after injection. Integrating the time-activity curves to find the area under the curve yields the Time Integrated Activity Coefficient (TIAC). The TIAC can be manually entered into OLINDA from excel or calculated directly in MIM's SurePlan MRT to find the dose to each OAR or lesion. In addition to an evaluation of each imaging protocol, the doses calculated from MIM and OLINDA will be compared as well.

4 Background

4.1 Lutetium

Lutetium is the seventy-first element on the periodic table and a lanthanide series metal. It is a solid at room temperature and is considered a rare earth metal. While Lutetium is known to have many isotopes, the main isotope of interest for this study is Lutetium-177. Lutetium-177(Lu-177 or $^{177}\mathbf{Lu}$) is a beta and gamma emitter with a half-life of 6.647 days according to the Brookhaven National Laboratory's National Nuclear Data Center(12). It emits a beta minus particle(83.47%) with a maximum energy of 496.8 keV and an average energy around 136.6 keV. Lu-177 is also a gamma emitter with energies of 112.9 (6.23%) and 208.4 keV (10.41%)(12). As both a beta minus and gamma emitter, Lu-177 can both serve as a therapeutic agent as well as ban imaging agent for a patient being imaged with SPECT, hybrid SPECT/CT, and/or planar imaging.

4.2 Radioactivity

Each element on the periodic table has at least one but often many isotopes. An isotope of an element shares the same number of protons, as this dictates an element's identity, and electrons, which allow the atom to have a neutral charge. An element's isotope is distinct in it's number of neutrons and effectively, atomic mass. The ratio of protons to neutrons in an isotope is used to predict its stability. When a nucleus is unstable, it decays into either a more stable isomeric transition with a different energy state or into another element. Since lutetium is neutron rich relative to the line of stability, it undergoes beta minus decay.(13)

Lutetium experiences two types of radioactive decay, beta minus decay and gamma decay. In beta minus decay, the decay scheme from parent nuclide X to daughter product Y is expressed as follows, ${}^{A}_{Z}\mathbf{X} \xrightarrow{\beta^-} {}^{A}_{Z+1}\mathbf{Y}$, with A being atomic mass number and Z being atomic number. In this simplified expression of a beta minus decay, a neutron converts to a proton with a beta minus particle, an anti-neutrino, and energy being released as well, show here:

$n^0 \rightarrow p^+ + e^- + \bar{\nu}+$ energy.

Following beta minus decay, ^{177}**Hf** decays into either the stable or metastable states of ^{177}**Hf** following the scheme $^{177}_{71}$**Lu** $\xrightarrow{\beta^-}$ $^{177}_{72}$**Hf**. ^{177}**Lu** has maximum beta energies of 497 keV(78.6%), 384 keV(9.1%), and 176 keV(12.2%). Isomeric transitions occurs through different mechanisms resulting in the ejection of a gamma ray photons from the atom of ^{177}**Hf**. Photons are emitted with the following energies from ^{177}**Hf**, 112.9 (6.17%) and 208.4 keV (10.36%). These two decay forms make ^{177}**Lu** an ideal radionuclide for nuclear medicine treatment as beta particle effectively provide tumor kill while gamma photons allow for SPECT and planar imaging of the distribution of radioactivity in a patient. The decay scheme is shown in more detail below.(14)

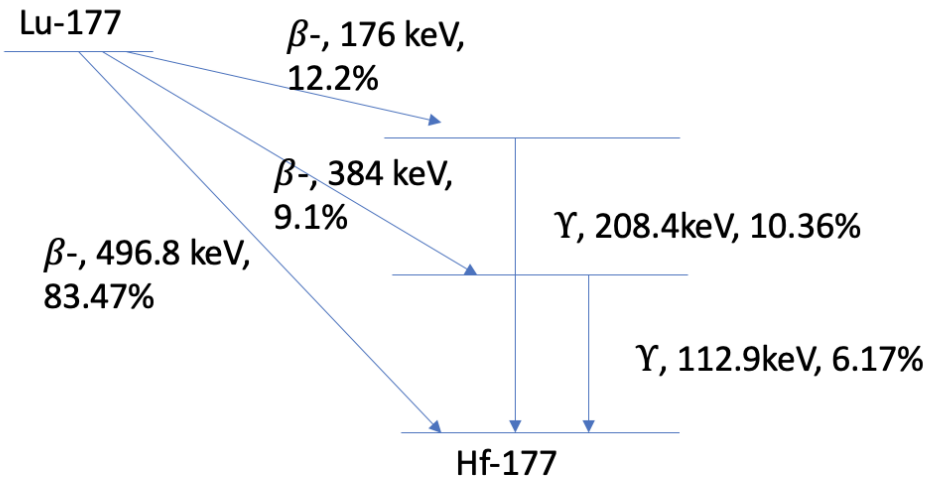

Figure 1: Decay Scheme of Lu-177 to Hf-177

4.3 Nuclear Medicine and Radiopharmaceuticals

Nuclear Medicine and Molecular imaging utilize radiopharmaceuticals to image and treat cancer. The decay mechanism of radioisotopes dictate whether they are more suitable for

imaging or treatment. Photon and positron(beta plus) decays are more suitable for imaging while alpha and beta minus decay is more useful for treatment. The pharmaceutical component of the radiopharmaceutical is used to guide the drug to its intended location providing precision treatment to specific types of cancer. Lutathera or Lu-177 Lu DOTATATE, has an affinity for somatostatin receptors on neuroendocrine tumors.(2) Lu-177 treats the tumors with beta particles while also emitting photons as part of this decay process. Individual radiopharmaceuticals or pairs of radiopharmaceuticals using different isotopes of the same element that have diagnostic and treatment capability contribute to the sub-field of theranostics in nuclear medicine. Theranostics is the combining of the terms Therapy and Diagnostics.(15) Not only can the pharmaceutical treat specific types of cancer but can also be located throughout the entire course of treatment. While some radiopharmaceuticals have the capability of of being both imaging and treatment agents, other theranostic agents utilize two isotopes of the same element to achieve this goal i.e. I-121 for imaging and I-131 for treatment. The true distribution and elimination half-life can be adequately visualized allowing for potential intervention or modification.

4.4 Radiation Biology

Ionizing radiation, which includes x-rays, gamma-rays, beta particles, and alpha particles, has the capability to damage cells as well as DNA when facilitated by free radicals. Damage is done to DNA in the form of single and double stand breaks where ionizing radiation collides with either one or both of the stands of DNA and chemically breaks the bonds between sequential nucleic bases in one or both stands, free radicals then fix the damage done by low LET radiation. When there is a single strand break in DNA there is little consequence in regard to the development of cancer. Since the other stand is left in tact and the complementary nucleic acid partner is present, standard reparation processes can commence. Essentially, a single strand break leaves a fully intact template to base the repair on. A double strand break gives way to more consequential changes in the structure of

the DNA. This is due to the fact that both of the nucleic base pairs are missing on their respective strands of DNA. There are several mechanisms of double stand break repair that utilized, however there is considerably more room for error.(13)

Several mechanisms are utilized by DNA to self-repair that occur in the late S phase or early G2 phase of DNA replication. These mechanisms include but are not limited to non-homologous end-joining, homologous recombination repair, crosslink repair, and mismatch repair. Each mechanism addresses a separate case of nucleic bases being present in the wrong order or paired with the wrong partner. For example, Mismatch repair is aptly named and corrects bases pairs that are not correctly matched. This repair is completed by Msh2-Msh6 or Msh2-Msh3 complexes that are uses to recognize the mismatch and recruit MLH1-PMSA2, MLH1-PMSA2M, and MLH1-MHL3 complexes to correct the mismatched pair. This process is catalyzed by exonuclease EXO1 and completed by polymerase δ/ϵ, RFC, and PCNA which adds back the correct base, completing the repair(13).

While there are several repair mechanisms in place to counter the effects, in the form of single and double strand breaks, caused by radiation radiation, the outcome is not always salvaged and fully repaired DNA. DNA exists in the shape of a double helix which can be radically modified when base pairs do not align, an incomplete repair occurs, or damage is sustained. In the field of biochemistry, it is taught that shape dictates function, meaning that if the overall shape of a strand of DNA is altered, it can longer code for protein synthesis or replicate effectively. When replication cannot be carried out as designed, either the new iteration of DNA transcribed in the DNA replication process resembles the damaged original DNA and continues to replicate in its damaged form or replication cannot occur and the cell housing the DNA will die. The latter option of failed replication leading to cell death is preferred. Cell death will prevent now mutated DNA from occupying generations of daughter cells. Generations of mutated and potentially further mutating daughter cells will not carry the proper function of the undamaged cell of the same type which can lead to the cell becoming cancerous. Different types of radiation have different amount of Linear

Energy Transfer (LET). LET is the measurement of energy deposition per unit distance. For example, α particles have a higher LET than photons. The amount of energy deposited per unit distance can affect how DNA is damaged since a strand of DNA is a finite distance. High LET radiation can deposit more energy in a very short track length that low LET radiation cannot. Differences in LET are one reason why absorbed dose is not an appropriate metric for radiation dose. To correct for the LET, charge, and mass differences in different types of radiation, the radiation specific weighting factor, w_R, takes into account how different types radiation affect tissue differently. The product of w_R and absorbed dose is refereed to as equivalent dose which is measured in Sieverts and also has units in Joules of energy per kilogram of mass. This factor exists to equate the dose difference when effected by the same amount of α particles and photons.

Equivalent dose is not the best metric either. Different organs have different levels of sensitivity to radiation than others. This has to do with their inherent makeup, whether they are serial or parallel organs, and/or how often their cells replicate. To take into account these inherent tissue differences, the tissue specific weighting factor, w_T, takes into account the different effect radiation has on different types of tissue. The product of w_T and equivalent dose is refereed to as effective dose. Effective dose, measured in Sieverts, scales the absorbed dose value to incorporate the effects of different types of radiation and different types of tissue.

4.5 Organs at Risk

Radiopharmaceuticals are used to treat specific regions of the body affected by cancer. The pharmaceutical portion of the radiopharmaceutical is used to transport the drug to the correct region of the body where the radionuclide can begin treating the cancerous tissue. The term Organs at Risk (OAR) refers to organs that are healthy and potentially affected by the pharmaceutical but are not intended to be treated.(13)(15) These organs serve as one of the limiting factors in treatment dose. While more radiation may be needed for effective

tumor kill, the OARs will also experience the increased level of radiation. Each OAR is different in its tolerance of radiation(16). Based on the degree of radiation tolerance and amount of dose distributed to an OAR a dose limit has to be established to ensure effective tumor kill without OAR toxicity.

4.6 Dosimetry and the MIRD Model

In terms of radiation, dose is defined as the energy imparted per unit mass. Even with this definition, it is difficult to actually quantify dose delivered from radiation in medicine. A standard of measurement and calculation of dose in nuclear medicine is provided by the Medical Internal Radiation Dose(MIRD) Committee of the Society of Nuclear Medicine and Molecular Imaging(SNMMI). The role of this committee is to outline the method at which radiation dose can be calculated a portion of which is published in the MIRD 21 Pamphlet(17).

As discussed earlier in background, each type of radiation does not effect tissue to the same extent nor dose each tissue experience the same amount of damage as other tissue from the same amount and type of radiation. Certain types of radiation are more damaging than others and certain types of tissues are more radiosensitive than others.

The MIRD pamphlet details the derivations necessary in calculating absorbed dose(D), equivalent dose(H), and effective dose(E). Absorbed dose is measured in Gray while effective and equivalent dose are measured in Sieverts. Each unit is equivalent to joules/kilogram, however effective and equivalent dose have additional unitless factors applied to convert from Gray to Sieverts.

Absorbed dose rate is a summation of the products of activity(A) and the radionuclide specific quantity(S) in units of Gray. This factor is patient specific in regard to sex, age, height, and mass(17)(18)(19). The dose rate applied to a region of tissue is expressed as

$$\dot{D}(r_T, t) = \sum_{r_s} A(r_s, t) S(r_t \leftarrow r_s, t) \tag{1}$$

where r_s is the radioactive source, r_T is the target of the radiation, and t is time elapsed. To calculated the mean absorbed dose, integration of the absorbed dose rate is required and is expressed as follows,

$$D(r_T, T_D) = \int_0^{T_D} \dot{D}(r_T, t)dt \tag{2}$$

$$D(r_T, T_D) = \int_0^{T_D} \sum_{r_s} A(r_s, t)S(r_t \leftarrow r_s, t)dt \tag{3}$$

The radionuclide specific quantity(S) is defined by MIRD 21 as

$$\begin{aligned} S(r_t \leftarrow r_s, t) &= \frac{1}{M(r_T, t)} \sum_i E_i Y_i \phi(r_t \leftarrow r_s, E_i, t) \\ &= \frac{1}{M(r_T, t)} \sum_i \Delta_i \phi(r_t \leftarrow r_s, E_i, t) \end{aligned} \tag{4}$$

where M is the mass of the target tissue as a function of time, E is the arithmetic mean energy of the radionuclide, Y is the ratio of number of nuclear transitions that occur for every nuclear transformation, and Δ is the product of E and Y. A nuclear transition is a reaction in which decay occurs in the isotope with the intention of releasing energy while a nuclear transformation is the change of one isotope of an element to an isotope of another element. For example Lu-177 can undergo a single beta decay transition when transforming to Hf-177 or it can undergo a beta decay and a gamma transition while transforming to Hf-177. In this equation, ϕ is the absorbed fraction which describes the ratio of energy emitted by the source that will be absorbed by the target at time t.

The formulation is similar for equivalent dose and effective dose. Equivalent dose equal to absorbed dose multiplied by a radiation specific weighting factor w_R which takes into account how different types radiation affect tissue differently. It can be expressed as

$$H(r_T, T_D) = \sum_R w_R D_R(r_T, T_D) \tag{5}$$

The same formulation applies to effective dose with the addition of the tissue specific weighting factor w_T which takes into account the different effect radiation has on every type of tissue and organ in the human body. It can be expressed as

$$E(r_T, T_D) = \sum_T w_T H_T(r_T, T_D) \tag{6}$$

The effects of concern determined by equivalent dose are stochastic. The relative biological effectiveness is used to predict deterministic effects. Intermediate steps as well as examples of application of these equations are detailed further in MIRD21(17).

4.7 Deterministic Effects

When discussing stochastic effects from radiation, absorbed dose is the metric of concern. For deterministic effects, that is, effects that are directly related to radiation dose, Biologically Effective Dose(BED)(20) and Relative Biological Effectiveness(RBE)(21) can be used to assess how soon a deterministic endpoint will be reached. The main deterministic effects of concern is acute myelosuppression and nephrotoxicity.(22)(1) These models factor in the different rates at which healthy or cancerous cells will be killed or spared by radiations of different LET. Relating absorbed dose to BED through RBE using the equation below aids clinicians in avoiding deterministic effects. The tissues of focus have set tolerances to avoid deterministic effects. The tolerances are 30 Gy for the liver, 23 Gy for the kidneys, and 40 Gy for the spleen. In future studies, bone marrow toxicity will be evaluated, the deterministic dose limit for bone marrow is 2-3 Gy.(16)

4.8 Imaging Modalities

4.8.1 Single Photon Emission Computed Tomography

The position and intensity of the photon emission distribution is important information as it delineates the uptake of Lutathera in the body. A Single Photon Emission Tomogra-

phy(SPECT) unit is composed of one to three panels of detectors that ostensibly form a bore around the patient. The panels are positioned in such a way that they can rotate around the patient while collecting data to create tomographic images that give a three-dimensional map of radionuclide distribution.

Scintillator detectors are used to collect the data of photon emission. In a scintillator detector, the first point of interaction for the gamma-ray photon is the scintillator crystal which converts the gamma-ray photon into visible light. The visible light then comes into contact with the photocathode, which converts the visible light into photoelectrons. A photoelectron is not sufficient at producing an adequate signal. This is rectified by the photomultiplier tube(PMT). The PMT takes the photoelectron and accelerates it over an electric potential generated by eight to eleven successive dynodes. Each sequential dynode has a constant potential difference and produces the same electrons gain with each interaction. The number of photoelectrons is increased by a consistent multiplication factor at each dynode, meaning the final numbers of electrons collected at the anode of the PMT, directly correlated to the number of incident gamma-ray photons initially incident of the scintillator crystal.(15)

Once the electrons reach the anode, the electronic signal enters the circuit and produces measurable data. SPECT is able to record the intensity of gamma-ray photon emission and produce a three-dimensional image to display this data. While the image created will give a rough estimate of which part of the body the radionuclide has traveled to, it does not provide exact delineation of distribution.(15). SPECT images, unlike planar imaging, avoid organ overlap and can therefore localize radionuclide uptake more effectively.

4.8.2 Planar Imaging

Planar Imaging utilizes the same technology as SPECT. The detector panels and detectors themselves are all positioned and function in the same way except for the fact that the gamma cameras remain stationary while the patient is slowly moved axially, creating a two-dimensional image. The image is often taken from an anterior-posterior view. This

modality can be done with the same unit as SPECT with the panels remaining stationary, or in a separate unit all together. Two-dimensional images are are acquired in a similar amount of time to SPECT and can provide a longer, albeit less quantitative axial field of view.(15)

4.8.3 Computed Tomography

Computed Tomography or CT scans offer a three-dimensionally reconstructed x-ray image of the patient. Like SPECT, CT positions an x-ray tube and x-ray detector on opposite sides of the bore where the patient lies. The combination of the x-ray tube and x-ray detector spin around the patient collection x-ray images that serve as projections of the anatomy that are reconstructed into a full three-dimensional image of the body.(15)

4.8.4 Hybrid Imaging

One of the nuclear medicine imaging modalities that is useful for imaging the distribution of Lutathera in the patient is SPECT/CT hybrid imaging. This modality is used to image radionuclides that emit single photons events during radioactive decay. As discussed earlier, there are several instances in the decay scheme of lutetium-177 where a single photon is ejected as hafnium-177 relaxes from an isomeric state. Hybrid imaging is the use of two or more imaging modalities fused together to overlay data that can be acquired with one of the modalities and not the other. In this case, SPECT and CT images are fused to produce images that show the distribution of the radionuclide from SPECT, overlaid on the anatomy imaged from CT. This provides a clear picture of radionuclide distribution within a clear boundary in the body.(15)

5 Methods and Materials

5.1 Methods

5.1.1 Imaging Protocol

An imaging protocol for Lutathera was designed based on a literature review of several clinics' proprietary protocols. The three main protocols that have been evaluated are intended to match the needs and capabilities of the OHSU Nuclear Medicine and Molecular Imaging Clinic. One is a more intensive, four time point protocol. This protocol includes a SPECT/CT scan on the day of treatment to establish a baseline, one SPECT/CT scan twenty-four hours post injecting, one SPECT/CT scan at day four after injection, and a late time-point at either day five or eight after injection. Contoured SPECT/CT images will be imported into MIM where integrated activity will be used to created TACs, calculate TIACs, generated Dose-Volume Histograms, and cumulative dose to each organ and lesion in Sureplan MRT and OLINDA.

This protocols below outline the specific parameters to configure a Whole Body Planar and SPECT units for this specific study. This includes the energy window, collimator, table speed, and acquisition matrix. Notably, the energy window is selected to be 208 keV with a tolerance of $\pm 10\%$. The lower energy decay is not included in this study as recommendation from two previous studies similarly attempting to provide patient-specific dosimetry for those being treated by Lutathera(23)(24). For this project, this protocol was not used nor will a protocol for whole body planar imaging be implemented. This is to highlight a future that will be implemented when OHSU recruits patients for this study which will utilize SPECT/CT.

	Scan 1	Scan 2	Scan 3
Photopeak	208.4 KeV	208.4 KeV	208.4 KeV
Energy Window	20 percent	20 percent	20 percent
Collimator	Medium Energy	Medium Energy	Medium Energy
Imaging Schedule	Within 24 hour post injection	96 hours post injection	168 hours post injection
Patient Preparation	Patient should be well hydrated and **void immediately before receiving dosimetric dose Patient should not void again until the end of scan 1**	Patient should be well hydrated and **void immediately prior to scan**	Patient should be well hydrated and **void immediately prior to scan**
Acquisition Matrix	256 x 1024	256 x 1024	256 x 1024
Scanning Rate	30cm/min	23cm/min	15cm/min
View	Anterior and Posterior whole body images should be acquired, including arms, from vertex through toes		

Figure 2: Specified Parameters for Whole Body Planar Imaging Protocol

	Scan 1	Scan 2	Scan 3
Photopeak	208.4 KeV	208.4 KeV	208.4 KeV
Energy Window	20 percent	20 percent	20 percent
Collimator	Medium Energy	Medium Energy	Medium Energy
Imaging Schedule	Within 24 hour post injection	96 hours post injection	168 hours post injection
Patient Preparation	Patient should be well hydrated and **void immediately before receiving dosimetric dose Patient should not void again until the end of scan 1**	Patient should be well hydrated and **void immediately prior to scan**	Patient should be well hydrated and **void immediately prior to scan**
Acquisition Matrix	128 x 128	128 x 128	128 x 128
Scanning Rate	30cm/min	23cm/min	15cm/min
View	SPECT Images from abdomen to pelvis, 360 degree rotation		

Figure 3: Specified Parameters for SPECT Imaging Protocol

5.1.2 Patients

The University of Michigan's Deep Blue Data Repository was utilized to preform patient specific dosimetry.(10) This allowed us to create test protocols by evaluating the dose calculated to OARs with different combinations of time-points without having to recruit patients to test different protocols. The data set supplied by University of Michigan included two patients with neuroendocrine tumors being treated by Lutathera, one male and one female. More details about each patient is supplied in the data set, including the patient six does not have a spleen and therefore dosimetry is not performed for that organ. The data consists of DICOM files that were imported into MIM. The RTStruct DICOM files contour the organs

at risk and the largest lesions in the patient. MIM's statistics viewer displayed the quantification of activity in the contoured regions, notable the Integral Total Activity Value. This value is plotted as a ratio to injected activity versus time to create time-activity curves. The timeline for treatment protocols is shown below, outlining the pre-treatment, treatment, and post-treatment timeline for diagnostic imaging occurrence.(25)

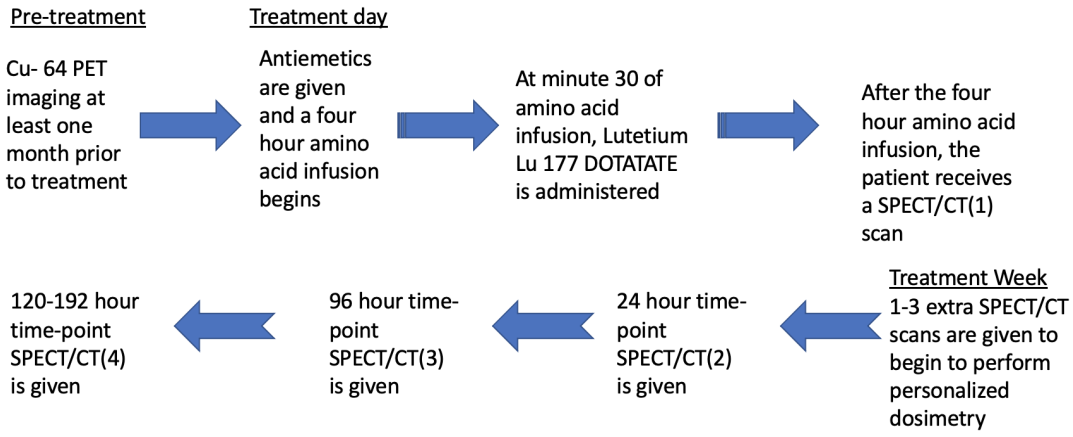

Figure 4: Timeline for Lutetium Lu 177 DOTATATE Treatment and Imaging Protocol

5.1.3 Data Processing

Segmentation on the CT and SPECT images yields average electron density and counts, respectively for a given region of interest. Electron density in Hounsfield Units is used for organ scaling in OLINDA or S value determination in MIM.

Counts from the SPECT image are needed to find activity, integrated activity, and lastly cumulative activity. To move from counts to activity in a given ROI, characterization must be completed on the SPECT unit. Characterization of a SPECT unit consists of taking a radioactive source, in this case lutetium 177, of known activity in a water phantom and measuring to determine the associated counts. Gamma cameras do not have 100% geometric sensitivity meaning that not all counts leaving the source will be detected due to the configuration of the camera. Additionally, the photons emitted will undergo attenuation and scatter in the body before reaching the SPECT unit, the water phantom exists to mimic a

human body. If all counts emitted by the radioactive source were detected by the gamma camera, the counts collected in a given interval would be equal the average activity over the given scan time. In actuality, the activity measured in that time frame will be less than the actual activity emitted by the source. Characterization of the SPECT unit quantifies correction factors to account for scatter, attenuation, geometric sensitivity, uniformity, etc. These factors allow for the counts detected to be scaled to match the activity of the radioactive source.

Once the SPECT unit undergoes characterization, the integrated activity in a given volume can be measured when segmentation occurs. To begin to calculate dose from integrated activity, a Time-Activity Curve is needed. Time-Activity Curves(TAC) detail the amount of activity present in a region as a function of time. For this calculation, this activity plotted is in a ratio with the activity injected. Integration of the time-activity curve with respect to time provides the TIAC which represents the cumulative activity present in the OAR or lesion over the total time the radionuclide is present in the body. As described in the background, MIRD21 provides abstract mathematical formulation for the calculation of dose to an OAR and lesion.

The TIAC can be exported to OLINDA in the units of Bq-hr/Bq, where the software calculates dose/injected activity with units of mSv/Bq using its library of RADAR stylized phantom-derived S-values. To avoid the need to open data on MIM, calculate TAC and TIAC in Excel, and finally dose/injected activity in OLINDA, MIM's SurePlan MRT Lutathera package allows for all computations to be conducted in one software. Newer versions of OLINDA as well as its image management and organ segmentation system HERMES, could also be utilized. The same aforementioned method of dose to OAR or lesion can be done through MIM's SurePlan MRT Lutathera package. This package contains a workspace that allows the user to import the contoured SPECT/CT images and automatically created TACs, calculates TIACs, generated Dose-Volume Histograms, source to target irradiated cumulative dose, and cumulative self-irradiated dose to each organ and lesion. SurePlan

MRT accomplishes these tasks through voxelized dosimetry. Voxelized dosimetry takes the activity value in a voxel which is a three-dimensional pixel, as well as the electron density in the same voxel and places this vector of values into a kernel. The kernel contains specific S-values for different amount of activity in different types of tissue. The vector input in the kernel corresponds with a dose output. Since this process is done voxel by voxel, more than the mean dose can be displayed. In addition to the mean dose, the maximum dose and dose value distribution is shown overlaid on the SPECT image as well as in a Dose Volume Histogram.

6 Results

The doses to organs at risk and tumors were evaluated in both MIM and OLINDA. The capabilities and outputs of both softwares vary and the data presented reflects that. MIM SurePlan MRT Lutathera package is able to create dose maps, Dose Volume Histograms, and Time-Activity curves. OLINDA 1.0 is only capable of producing dose/injected activity with units of mSv/Bq using its library of RADAR stylized phantom-derived S-values for each organ with the additional capability of scaling the calculation based on organ volume. The additional calculation for OLINDA were completed in excel including the calculation of time-integrated activity curves and dose to organs at risk.

6.1 MIM

The below Dose Volume Histograms with accompanying dose maps from MIM displays the percentage of volume of tissue that received at least a certain dose and the minimum dose received by a percentage of volume. The Dose Volume Histograms shown, in order, display the doses calculated using the four, three, and single time point protocols that are being evaluated. As the data set utilizes four time points, the three and single time point scans are simulated by the exclusion of data. For the three time point protocol, the day zero scan is omitted and for the single time point, the day one and final scans are omitted. The accompanying images of the dose distribution are screen captured meant to show another feature of MIM, three dimensional dose mapping. On the software itself, the user can scroll through the image set.

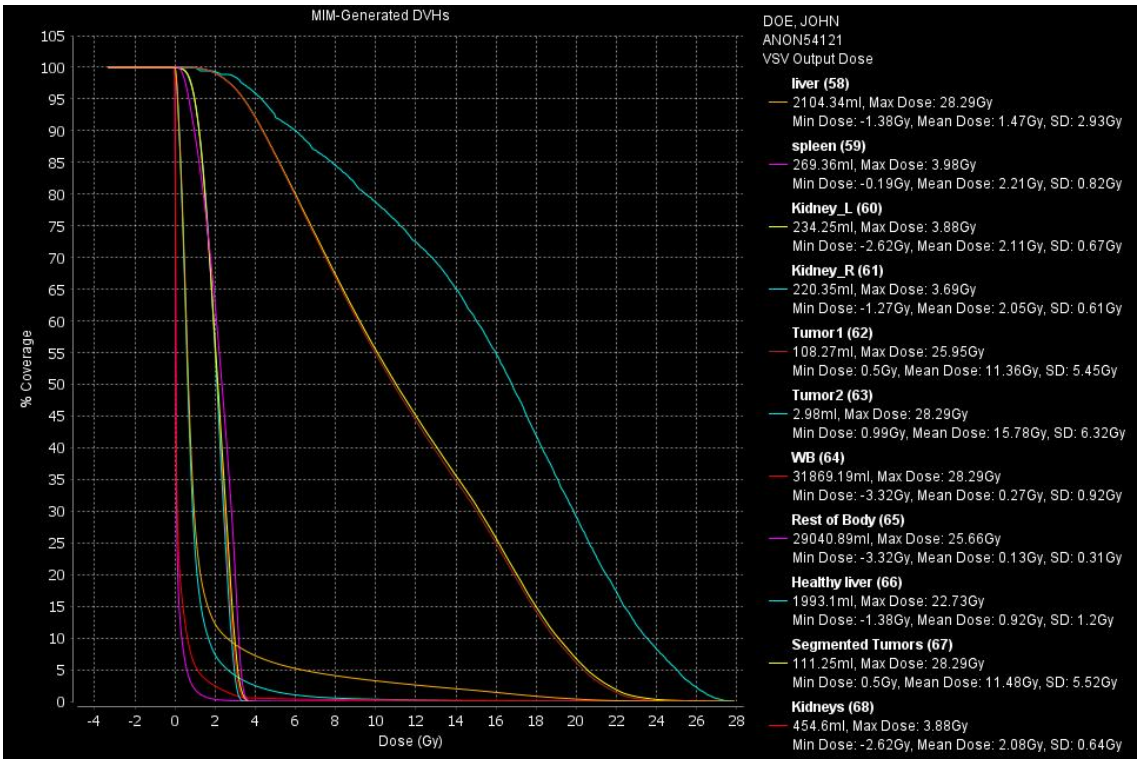

Figure 5: Four time-point Dose Volume Histogram for Patient 4

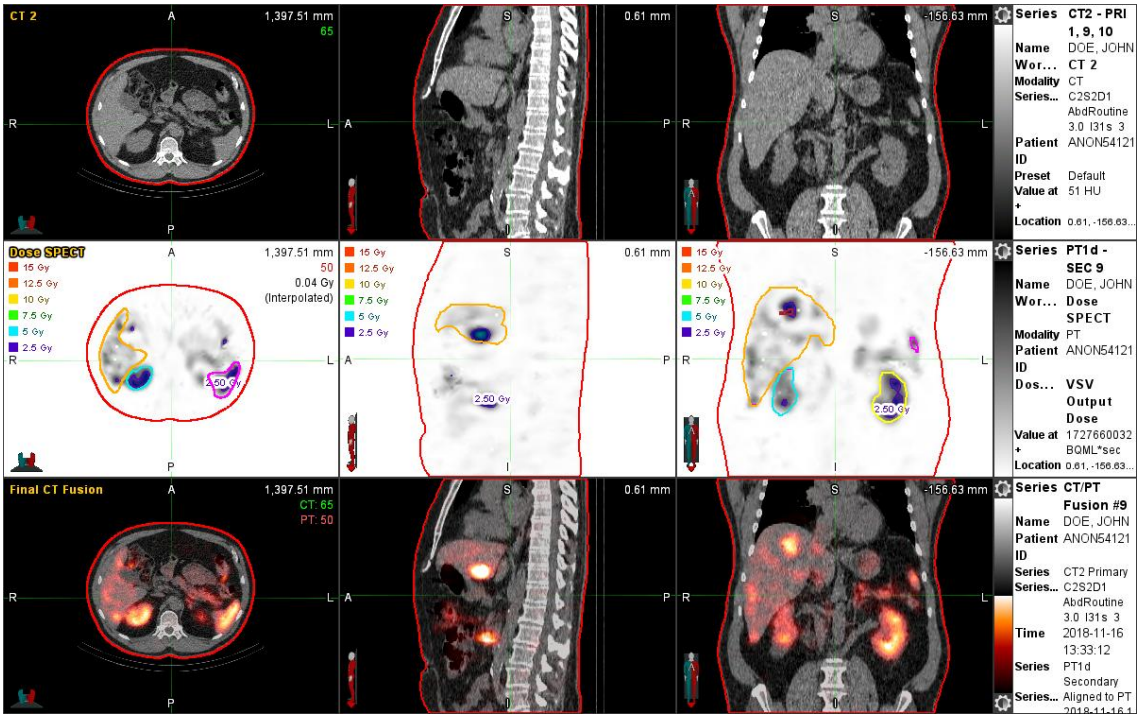

Figure 6: Four time-point Fused Images for Patient 4

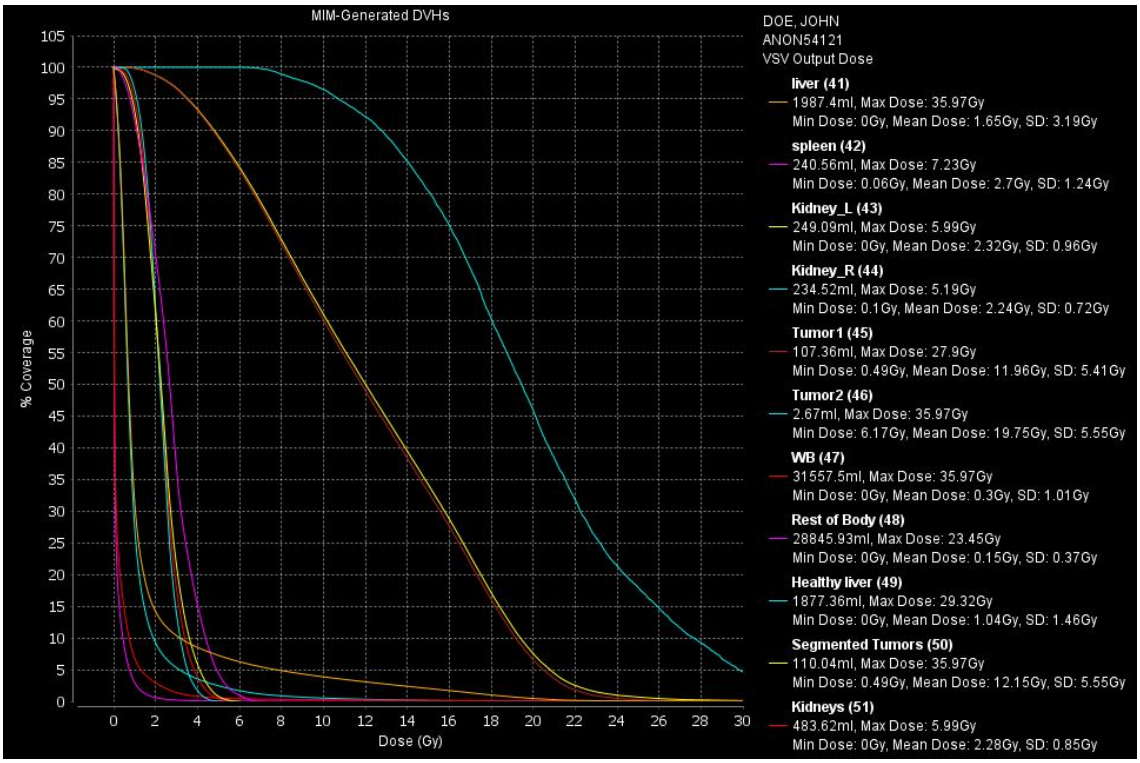

Figure 7: Three time-point Dose Volume Histogram for Patient 4

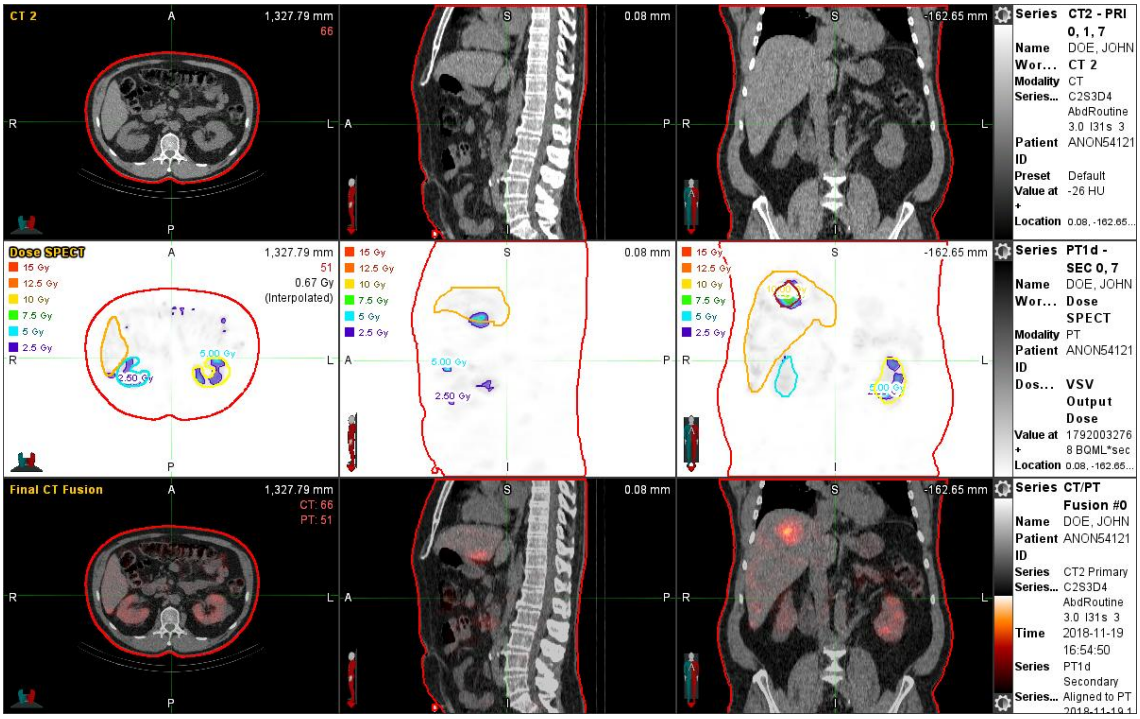

Figure 8: Three time-point Fused Images for Patient 4

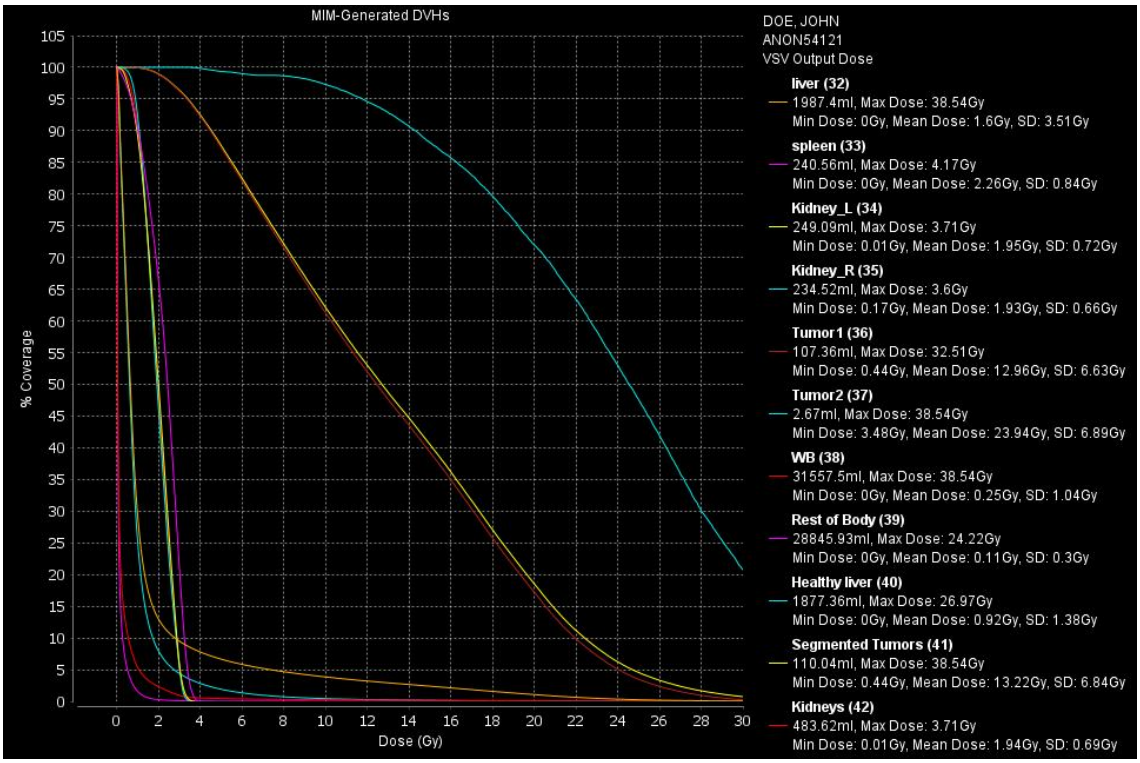

Figure 9: Two time-point Dose Volume Histogram for Patient 4

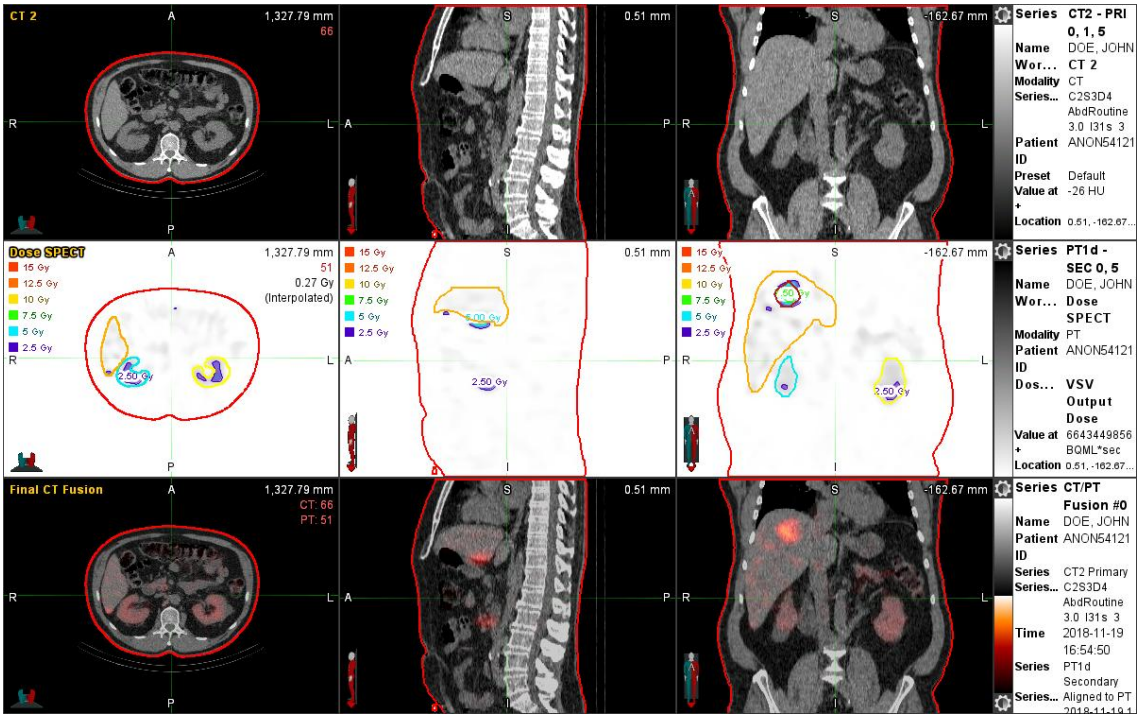

Figure 10: Two time-point Fused Images for Patient 4

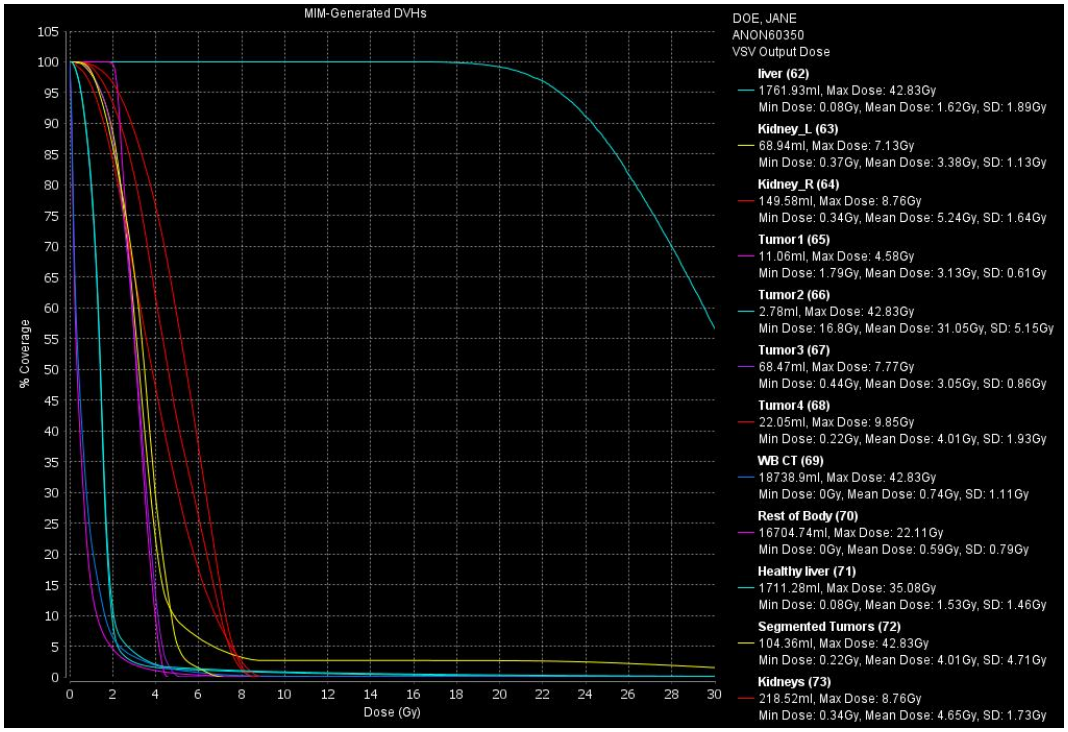

Figure 11: Four time-point Dose Volume Histogram for Patient 6

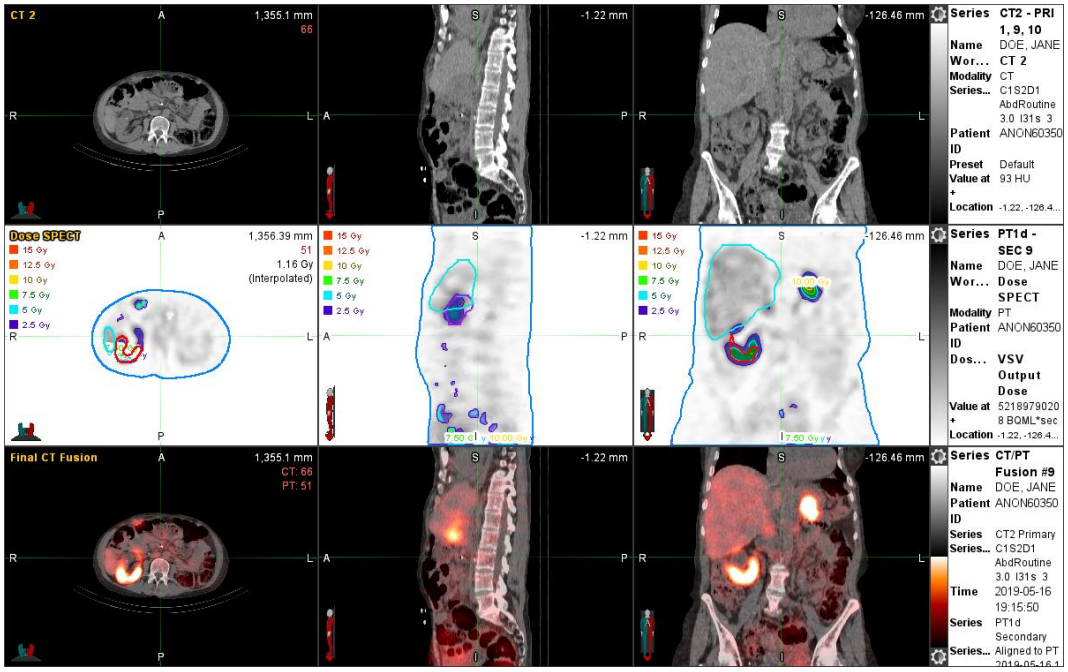

Figure 12: Four time-point Fused Images for Patient 6

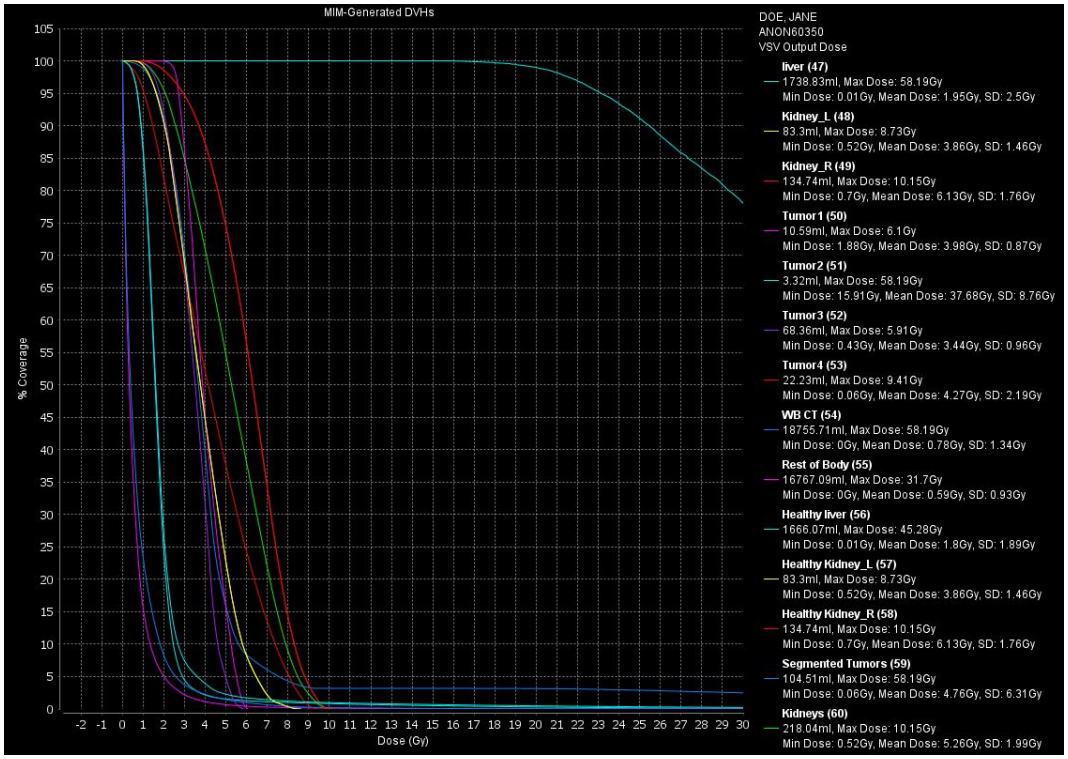

Figure 13: Three time-point Dose Volume Histogram for Patient 6

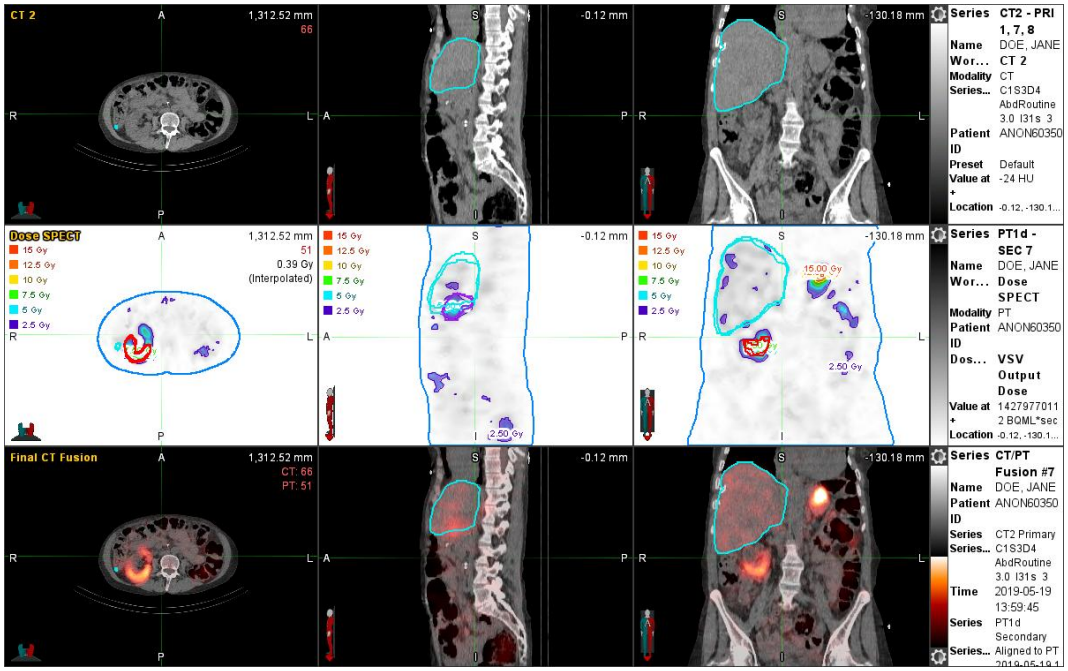

Figure 14: Three time-point Fused Images for Patient 6

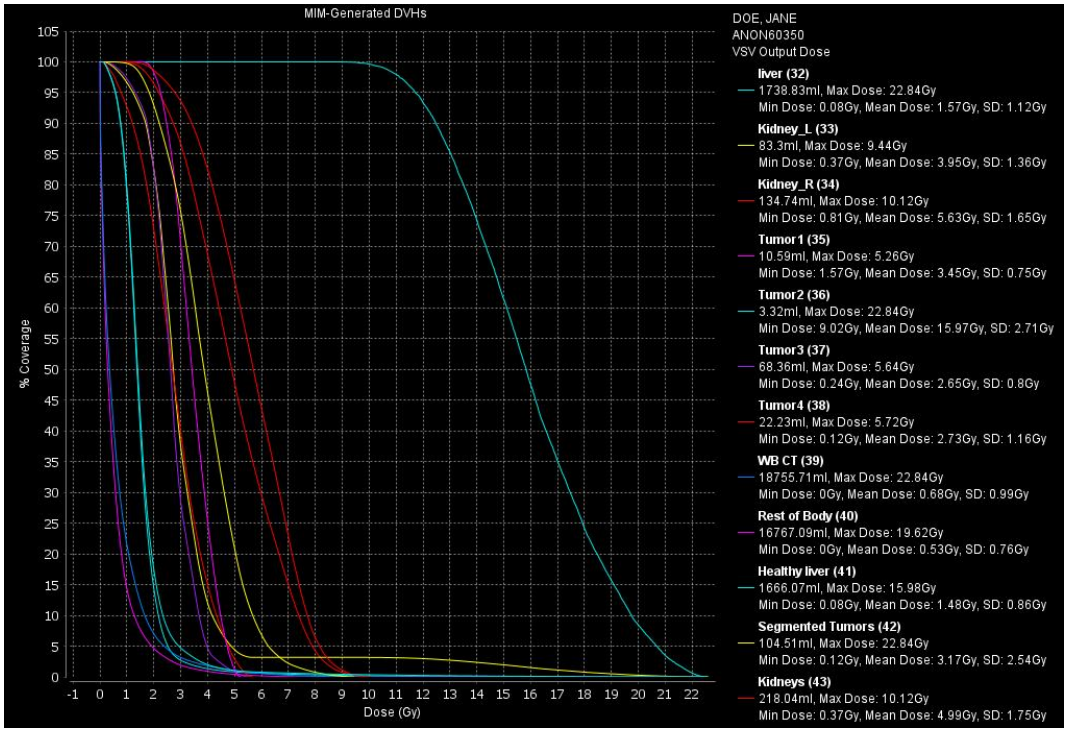

Figure 15: Two time-point Dose Volume Histogram for Patient 6

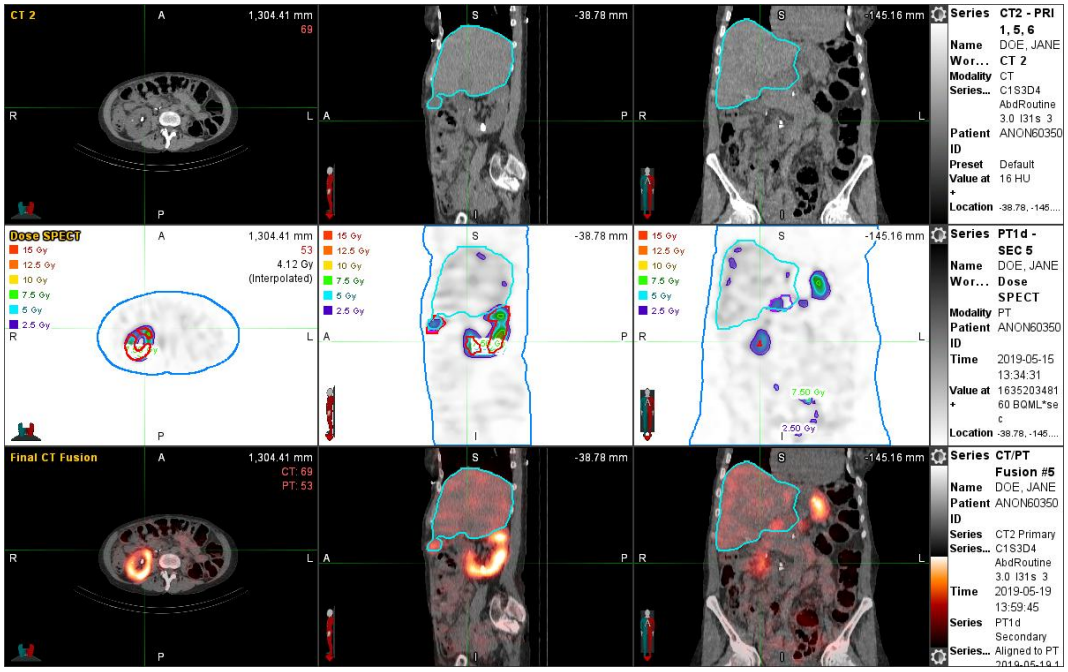

Figure 16: Two time-point Fused Images for Patient 6

6.2 MIM Time point Comparisons

The dose difference was calculated compared to the four time-point protocol for both the three and single time-point protocols. The four time-point protocol is used as the standard of comparison as its data points accurately represent the uptake and clearance times for lutathera.

Table 1: Patient 4

four time-points

organ	MIM dose(Gy)
liver	1.52
kidneys	2.66
spleen	3.28

three time-points

organ	MIM dose(Gy)	percent difference
liver	1.56	2.63
kidneys	2.69	1.12
spleen	3.31	0.914

two time-points

organ	MIM dose(Gy)	percent difference
liver	1.42	-6.57
kidneys	2.68	0.75
spleen	3.29	0.30

Table 2: Patient 6

Four Time-Points		
organ	MIM dose(Gy)	
liver	1.53	
kidneys	4.65	
Three Time-Points		
organ	MIM dose(Gy)	percent difference
liver	1.8	17.64
kidneys	5.26	13.11
Two Time-Points		
organ	MIM dose(Gy)	
liver	1.48	-3.26
kidneys	4.99	7.31

6.3 Time Point Activity and Time Integrated Activity Curves

The Integral Total Activity is used both in the MIM and OLINDA calculation. The values themselves come from MIM's contouring and statistics package. As this data is propitiatory to MIM, the calculation is done with a specific workflow. For OLINDA 1.0, a secondary software, in this instance excel, was used to calculate the Time Integrated Activity Curves which provided the input values for OLINDA to calculate dose. The Time Integrated Activity Curves were fitted using the least-squares fitting model which transforms exponential equations $y = C * e^{kx}$ into a linear equation,$\ln(y) = \ln(C) + kx$, before applying the fit. Wolfram Mathword© provides a detailed description of the process. These input values have the units Becquerel*hour per Becquerel. Tables one and five below represent the Integral Total Activities at given times in each organ at risk for patients 4 and 6 respectively.

Tables two-four for patient four and six-eight for patient six show the time integrated activity curve value for each organ for each time point protocol.

Table 3: Integral Total Activity(BQML*ml) at each time-point: Patient 4

patient ID: 4

scan number	time elapsed(hr)	liver	kidney total	spleen
1	3.741	289327059	191146591.9	84645612.52
2	27.73	218526458.3	141607335.3	78529575.72
3	103.1	123865668.2	49053672.99	34693509.3
4	124	116527440.8	35052638.02	27874472.4

Table 4: Time Integrated Activity Curve: Four-Time Points

patient 4

organ	negative decay constant	Ln(A)	A	TIAC
liver	-0.007568861	-3.23600489	0.039320672	5.1950577
kidneys	-0.014087476	-3.55860489	0.028478528	2.0215493
spleen	-0.009675003	-4.33875232	0.013052804	1.34912663

Table 5: Time Integrated Activity Curve: Three Time-Points

patient 4

organ	negative decay constant	Ln(A)	A	TIAC
liver	-0.0068	-3.31766	0.036238	5.330226
kidneys	-0.01439	-3.52692	0.029395	2.043269
spleen	-0.01078	-4.2216	0.014675	1.361298

Table 6: Time Integrated Activity Curve: Two Time-Points

patient 4

organ	negative decay constant	Ln(A)	A	TIAC
liver	-0.00854	-3.18372	0.041431	4.852359
kidneys	-0.01369	-3.57897	0.027904	2.03845
spleen	-0.00898	-4.41117	0.012141	1.352492

Table 7: Integral Total Activity(BQML*ml) at each time point: Patient 6

patient ID: 6

scan number	time elapsed(hr)	liver	kidney total	spleen
1	3.8	236430176	113761892	N/A
2	28.8	205486384	118563346	N/A
3	95.82	105933168	46229340	N/A
4	189.5	47931664	14457662.75	N/A

Table 8: Time Integrated Activity Curve: Four Time-Points

patient 6

organ	negative decay constant	Ln(A)	A	TIAC
liver	-0.008786227	-3.36776	0.034467	3.922797
kidneys	-0.011794831	-3.95595	0.019141	1.62279

Table 9: Time Integrated Activity Curve: Three Time-Points

patient 6

organ	negative decay constant	Ln(A)	A	TIAC
liver	-0.00902	-3.33322	0.035678	3.955424
kidneys	-0.01305	-3.77045	0.023042	1.765606

Table 10: Time Integrated Activity Curve: Two Time-Points

patient 6

organ	negative decay constant	Ln(A)	A	TIAC
liver	-0.00872	-3.39819	0.033434	3.832082
kidneys	-0.00979	-4.1257	0.016152	1.650559

6.4 Time-Activity Curves

The graphs in this section are the Time-Activity Curves for each organs at risk evaluated for each patient using the three imaging protocols. These graphs display the exponential trend line with accompanying R^2 value calculated by excel to model the effective decay of activity in the patient. The time-activity curves graphically display what was integrated using the least-squares approximation method to find the Time Integrated Activity Curves in the previous subsection.

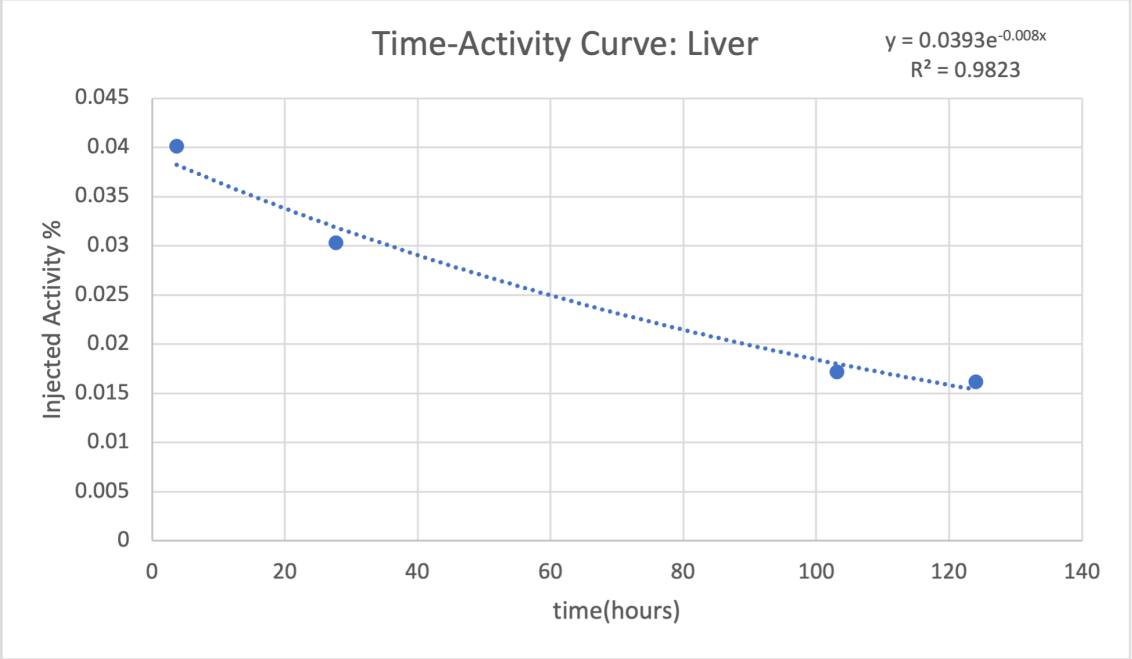

Figure 17: Four time point Time-Activity Curve of Liver for Patient 4

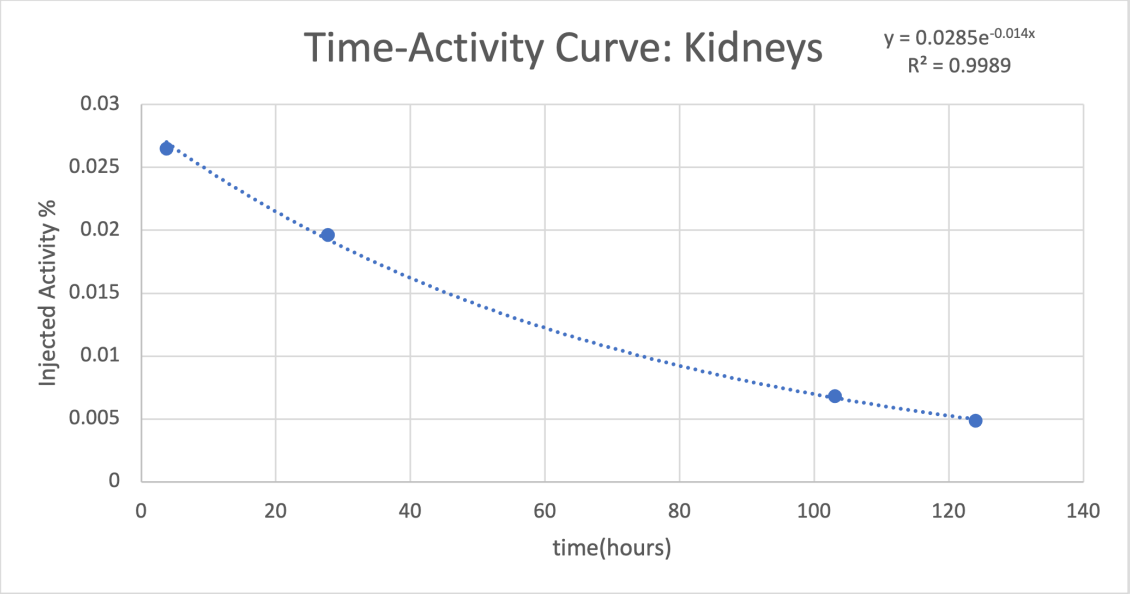

Figure 18: Four time point Time-Activity Curve of Kidneys for Patient 4

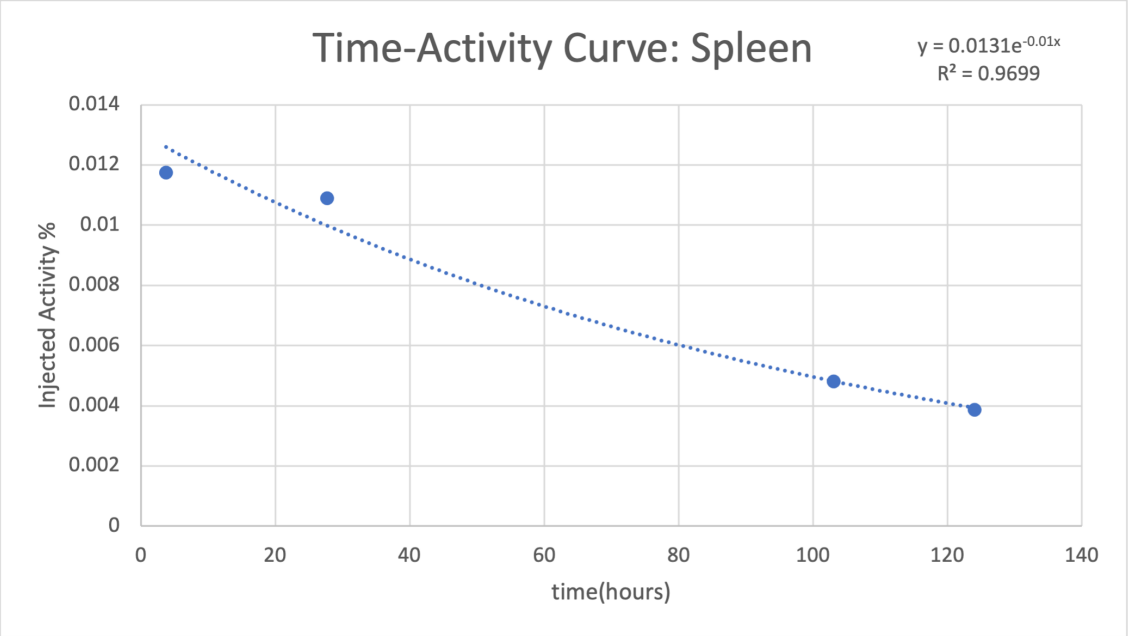

Figure 19: Four time point Time-Activity Curve of Spleen for Patient 4

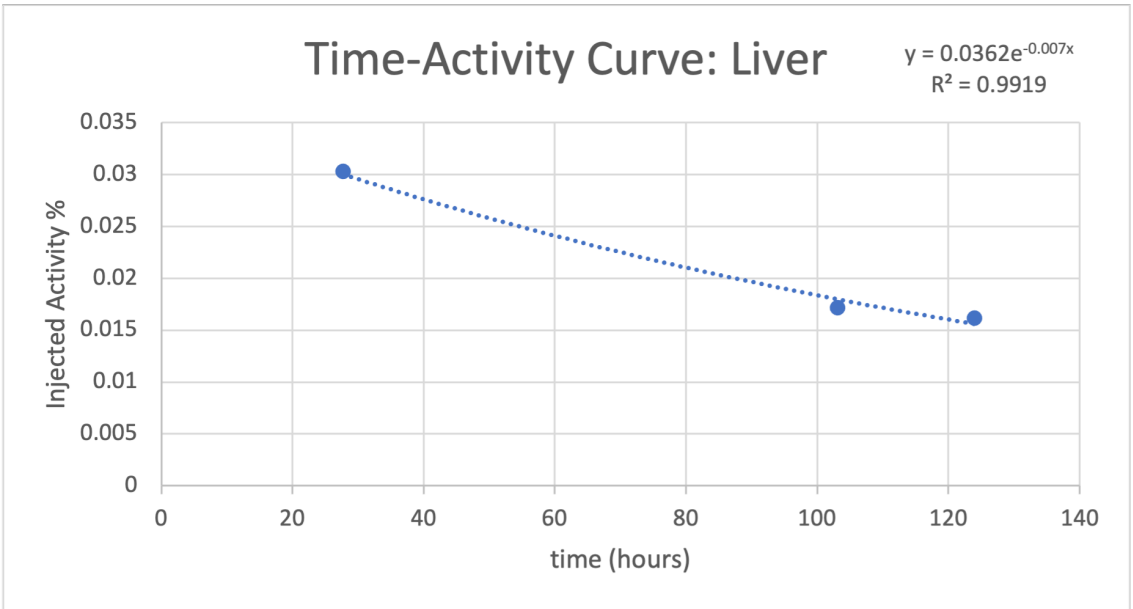

Figure 20: Three time point Time-Activity Curve of Liver for Patient 4

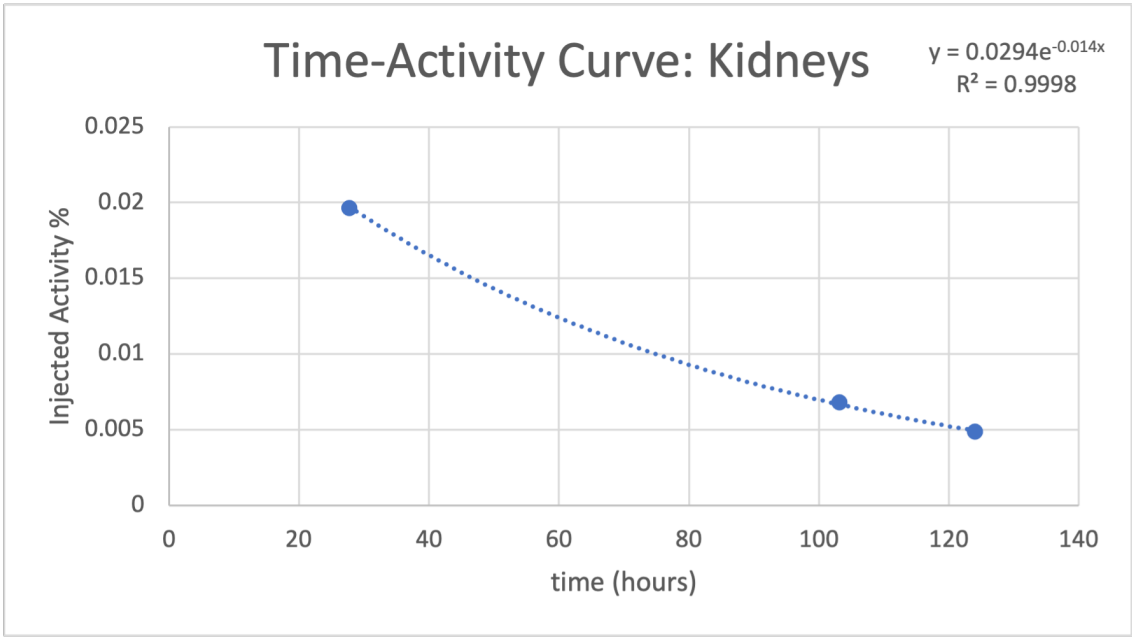

Figure 21: Three time point Time-Activity Curve of Kidneys for Patient 4

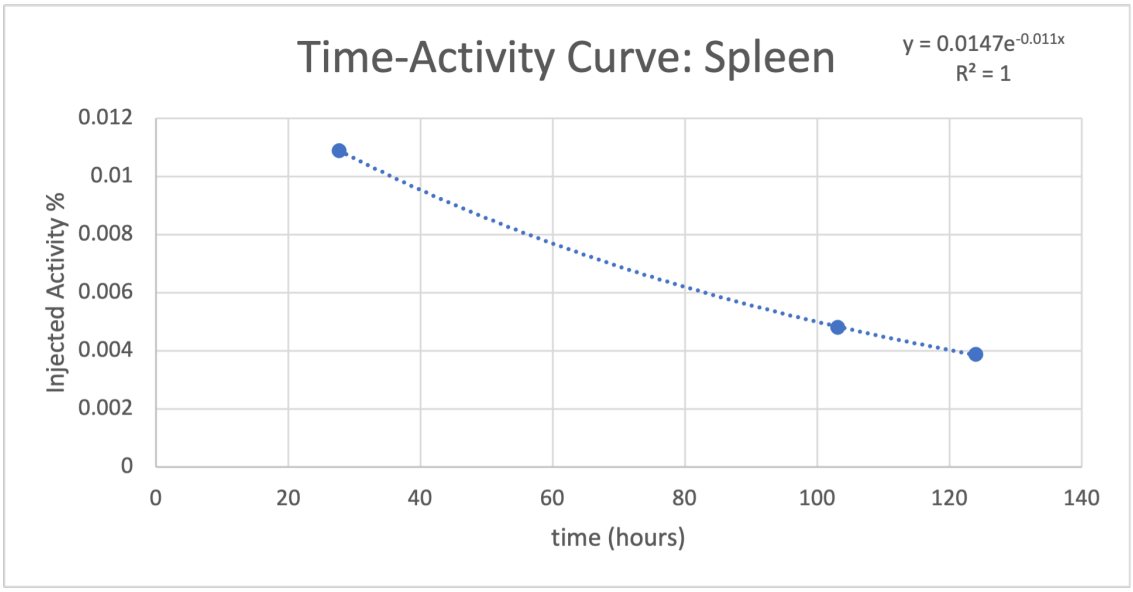

Figure 22: Three time point Time-Activity Curve of Spleen for Patient 4

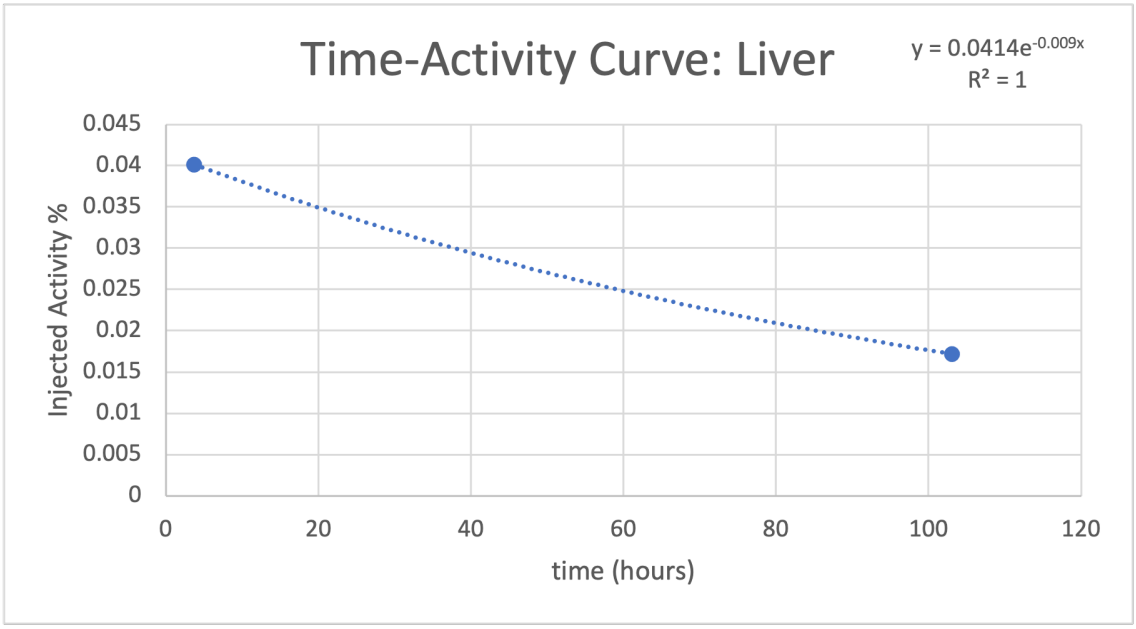

Figure 23: Two time point Time-Activity Curve of Liver for Patient 4

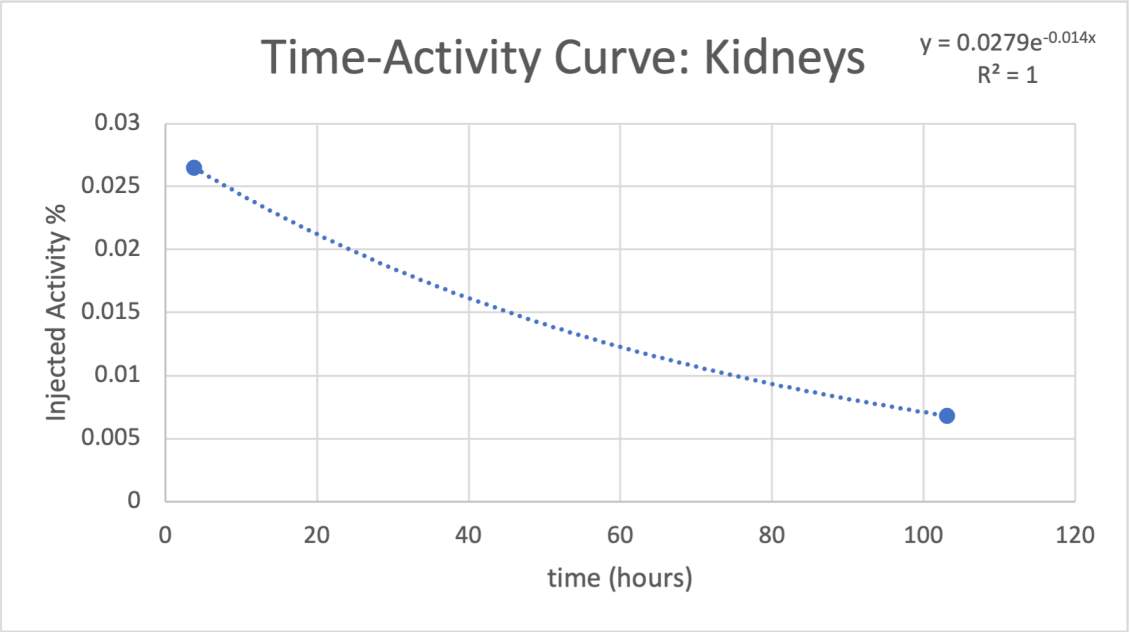

Figure 24: Two time point Time-Activity Curve of Kidneys for Patient 4

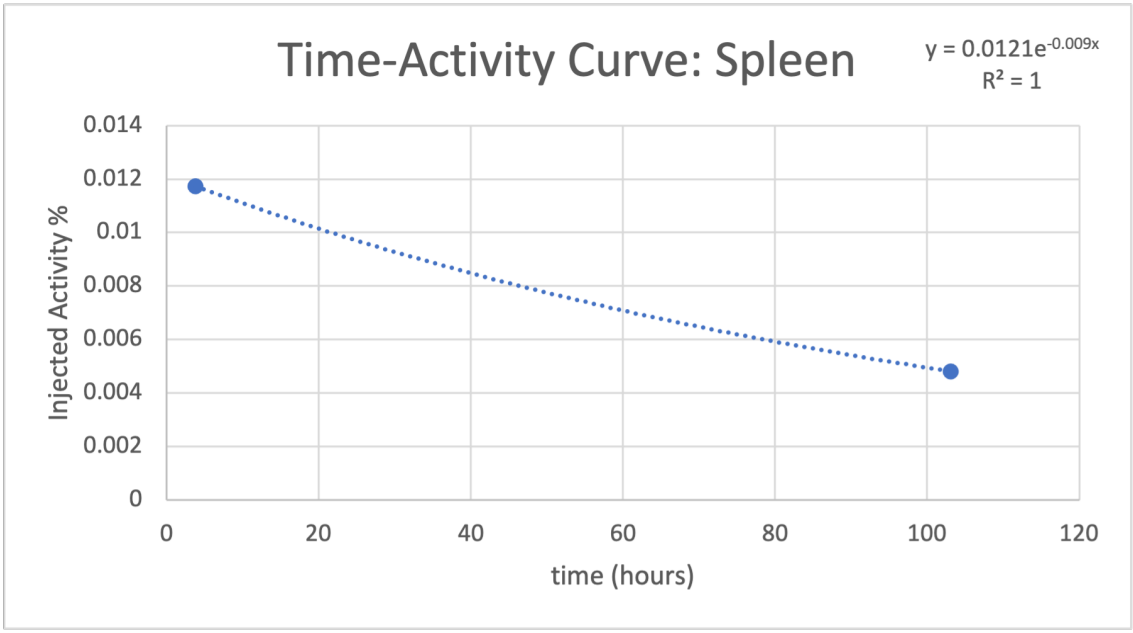

Figure 25: Two time point Time-Activity Curve of Spleen for Patient 4

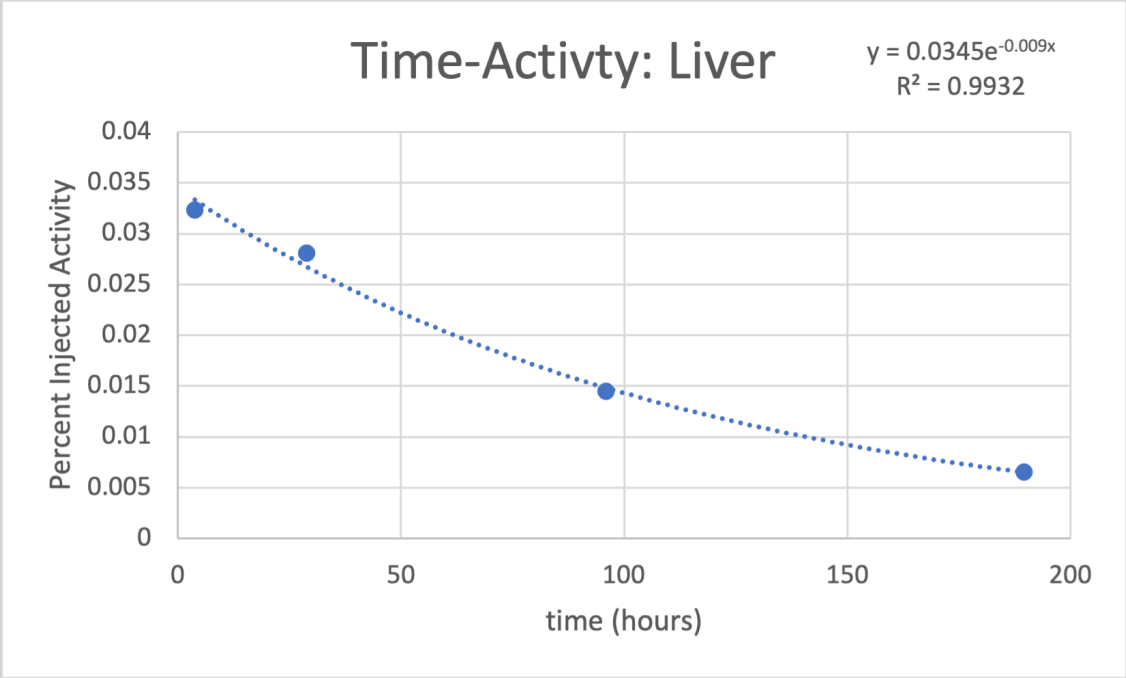

Figure 26: Four time point Time-Activity Curve of Liver for Patient 6

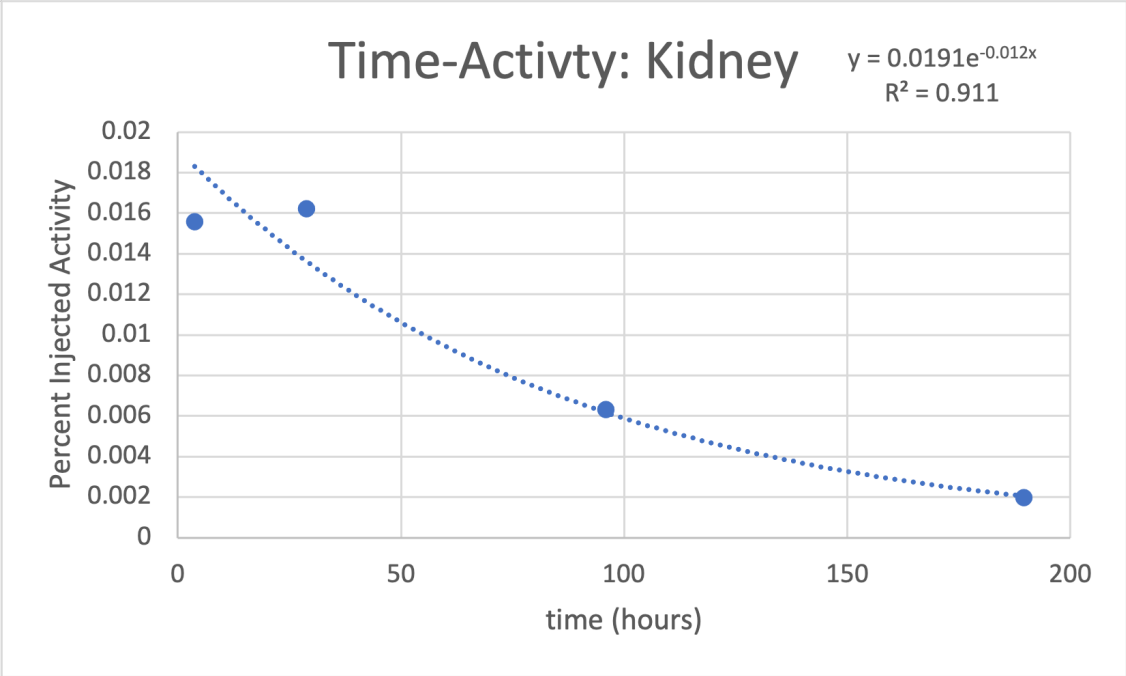

Figure 27: Four time point Time-Activity Curve of Kidneys for Patient 6

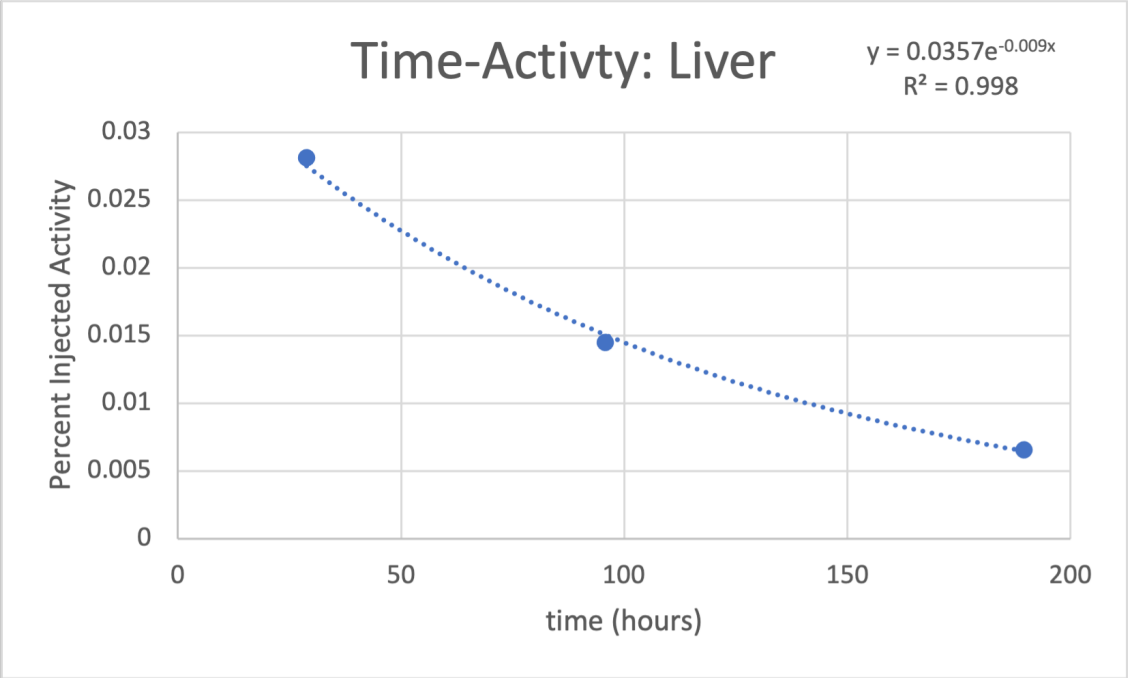

Figure 28: Three time point Time-Activity Curve of Liver for Patient 6

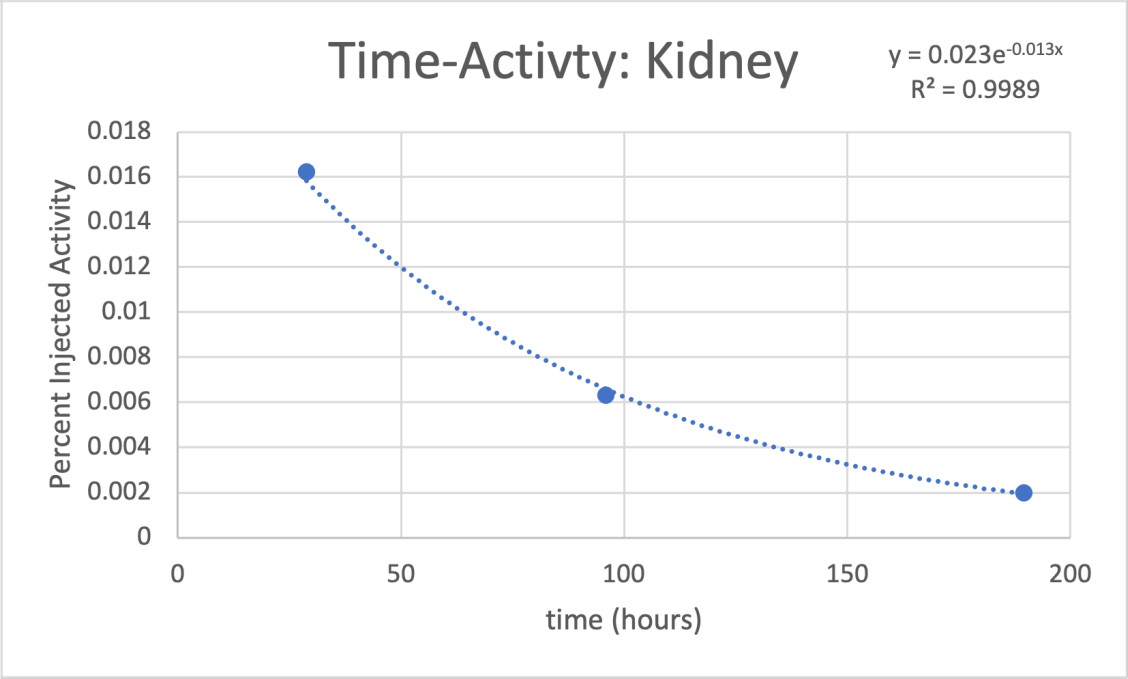

Figure 29: Three time point Time-Activity Curve of Kidneys for Patient 6

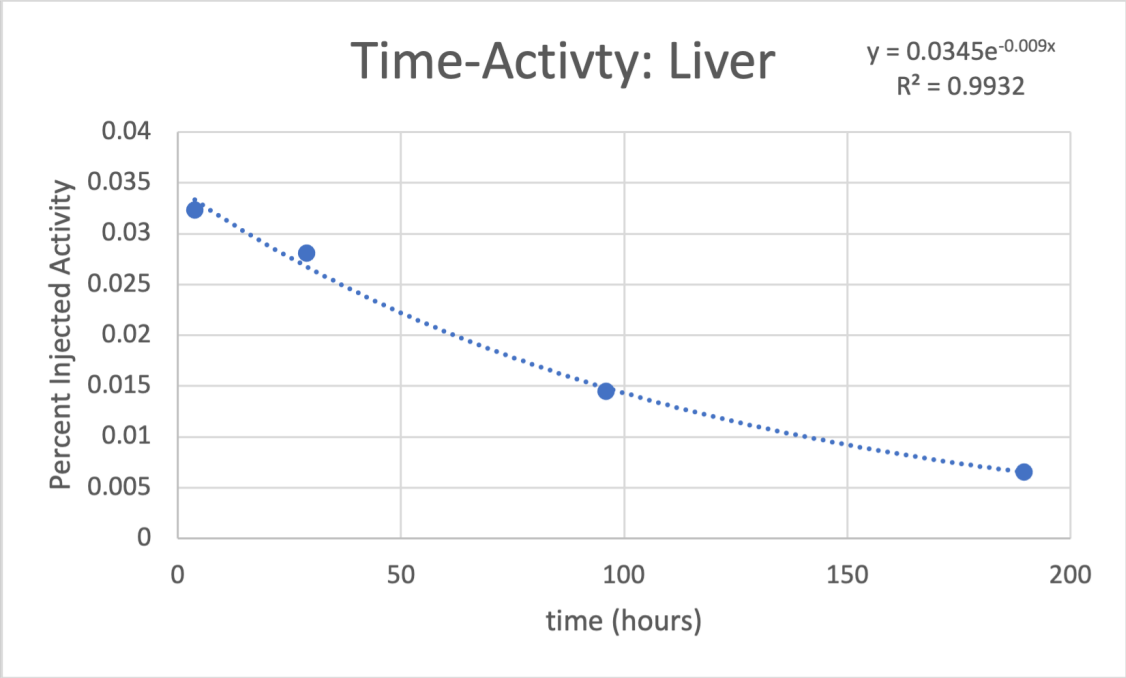

Figure 30: Two time point Time-Activity Curve of Liver for Patient 6

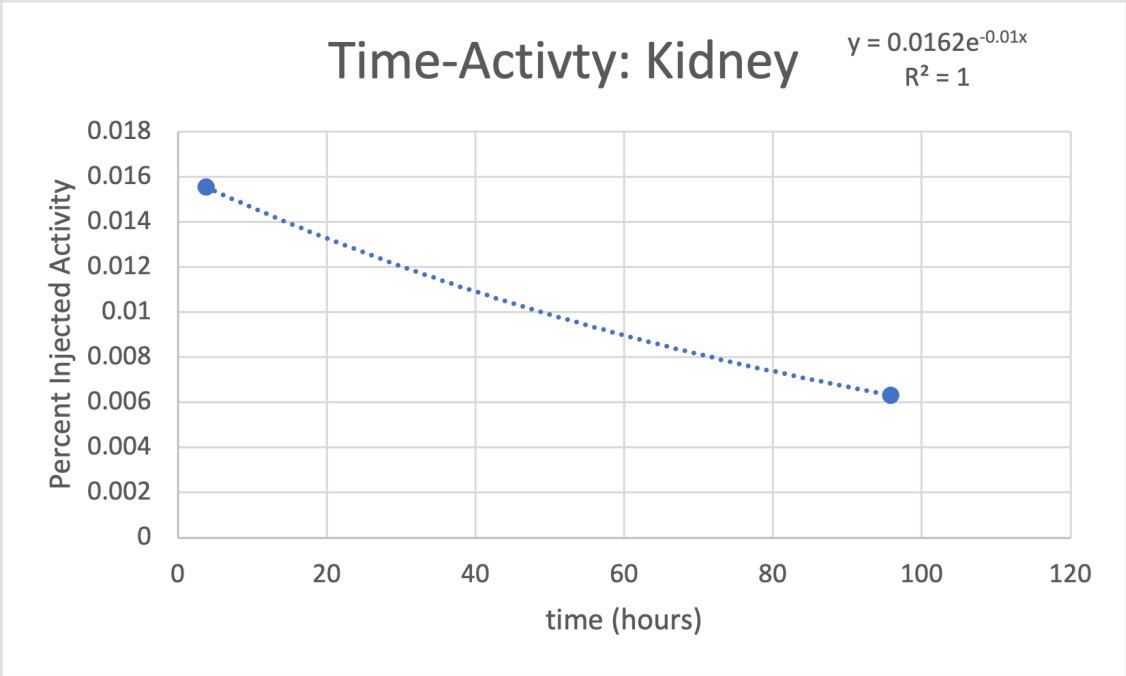

Figure 31: Two time point Time-Activity Curve of Kidneys for Patient 6

6.5 Doses Calculated through OLINDA

In order to tailor dosimetry for an individual patient in OLINDA, mass corrections for each organ needed to be imported into OLINDA to modify the makeup of the dosimetry phantom. Tables eleven and eighteen detail the masses needed. OLINDA did not output the absorbed doses themselves, only the absorbed dose per unit activity. These were converted to absorbed dose and compared to dose limits in Tables twelve-seventeen for patient four and nineteen-twenty-four for patient 6. In addition to doses and dose limits, the dose difference was calculated compared to the four time point protocol for both the three and single time point protocols. The four time-point protocol is used as the standard of comparison as its data points accurately represent the uptake and clearance times for lutathera.

Table 11: Mass Correction for OARs for Patient 4

organ	HU	density(g/mL)	volume(mL)	mass(g)
liver	53.53	1.05353	2068.865	2179.611
rkidney	17.73	1.01773	228.715	232.7701
lkidney	18.29	1.01829	238.5775	242.9411
kidneys			467.2925	475.7112
spleen	40.96	1.04096	247.485	257.622

Table 12: OLINDA output of Absorbed Dose per injected Activity for Four-Time Point Protocol

Four time points	
organs	OLINDA output(mSv/MBq)
liver	2.12E-01
kidneys	3.70E-01
spleen	4.56E-01

Table 13: Absorbed dose and Absorbed Dose Limits for OARs for Four-Time Points

dose to organ(mSv)	organ limit(mSv)
1528.52	30000
2667.70	23000
3287.76	40000

Table 14: OLINDA output of Absorbed Dose per injected Activity for Three-Time Point Protocol

organs	OLINDA output
liver	2.17E-01
kidneys	3.74E-01
spleen	4.60E-01

Table 15: Absorbed dose and Absorbed Dose Limits for OARs for Three-Time Points

dose to organ(mSv)	organ limit(mSv)	percentage deviation from Four-time point dose
1564.57	30000	2.35
2696.54	23000	1.08
3316.60	40000	0.87

Table 16: OLINDA output of Absorbed Dose per injected Activity for Two-Time Point Protocol

organs	OLINDA output
liver	1.31E-01
kidneys	2.83E-01
spleen	3.08E-01

Table 17: Absorbed dose and Absorbed Dose Limits for OARs for Two-Time Points

dose to organ(mSv)	organ limit(mSv)	percentage deviation from Four-time point dose
1427.58	30000	-6.60
2689.33	23000	0.81
3294.97	40000	-6.60

Table 18: Mass Corrections for Patient 6

organ	HU	density(g/mL)	volume(mL)	mass(g)
liver	53.68	1.05368	1707.53	1799.19
rkidney	19.98	1.01998	152.055	155.0931
lkidney	15.4	1.0154	76.7525	77.93449
kidneys			228.8075	233.0275

Table 19: OLINDA output of Absorbed Dose per injected Activity for Four Time-Point Protocol

Four time points	
organs	OLINDA output(mSv/MBq)
liver	1.89E-01
kidneys	6.13E-01

Table 20: Absorbed dose and Absorbed Dose Limits for OARs for Four-Time Point

dose to organ(mSv)	organ limit(mSv)
1381.59	30000
4481.03	23000

Table 21: OLINDA output of Absorbed Dose per injected Activity for Three Time-Point Protocol

Three time points	
organs	OLINDA output(mSv/MBq)
liver	1.95E-01
kidneys	6.55E-01

Table 22: Absorbed dose and Absorbed Dose Limits for OARs for Three Time-Point

dose to organ(mSv)	organ limit(mSv)	percentage deviation from 4 time-point dose
1425.45	30000	3.17
4788.05	23000	6.85

Table 23: OLINDA output of Absorbed Dose per injected Activity for Two-Time Point Protocol

Single Time point with baseline	
organs	OLINDA output(mSv/MBq)
liver	1.89E-01
kidneys	6.13E-01

Table 24: Absorbed dose and Absorbed Dose Limits for OARs for Two-Time Points

dose to organ(mSv)	organ limit(mSv)	percentage deviation from 4 time-point dose
1381.59	30000	0
4481.03	23000	0

6.6 MIM and OLINDA Comparison

MIM and OLINDA both have the capability of providing organ specific dosimetry with different methods. Given the same input data, table twenty-five shows the comparison in dosimetric calculations computed in both softwares for patient four.

Table 25: Patient 4

time points	organ	OLINDA dose(Gy)	MIM dose(Gy)	percent difference
4	liver	0.97	1.52	35.96
	kidneys	2.04	2.66	23.29
	spleen	2.27	3.28	30.75
3	liver	0.95893	1.56	38.53
	kidneys	2.06927	2.69	23.07
	spleen	2.36488	3.31	28.55
1	liver	0.94451	1.42	33.48
	kidneys	2.04043	2.68	23.86
	spleen	2.22068	3.29	32.50

Table 26: Patient 6

time-points	organ	OLINDA dose(Gy)	MIM dose(Gy)	percent difference
4	liver	1.38	1.53	-9.80
	kidneys	4.48	4.65	-3.65
3	liver	1.42	1.8	-21.11
	kidneys	4.78	5.26	-9.12
2	liver	1.38	1.48	-6.75
	kidneys	4.48	4.99	-10.22

7 Discussion

Personal Dosimetry can provide a more precise medical treatment to those receiving the medication. The goal of this evaluation is to determine the most effective and efficient protocol to provide personal dosimetry for lutathera. The standard of comparison is the four time point protocol where imaging takes place on day zero, day one, day four, and either day five or eight. As this may not be the most feasible protocol, a protocol omitting the day zero time point and another protocol excluding the day one and day five/eight time point are compared.

The first objective of this project was to evaluate the differences in dose calculated to each organ at risk given three time-point protocols. For patient four using MIM it was found that compared to the four time-point protocol, the percentage differences in dose calculated for the three time-point protocol were 2.63% and for the liver, 1.12% for the kidneys, and 0.914% and for the spleen. The percentage differences in dose calculated for the two time-point protocol were 0-6.57% for the liver, 0.75% and for the kidneys, and 0.30% and for the spleen.For patient six using MIM it was found that compared to the four time-point protocol, the percentage differences in dose calculated for the three time point protocol were 17.64% and for the liver and 13.11% for the kidneys. The percentage differences in dose calculated for the two time-point protocol were -3.26% and for the liver and 7.31% for the kidneys.

The first objective was also evaluated through OLINDA. For patient four it was found that compared to the four time-point protocol, the percentage differences in dose calculated for the three time-point protocol were 2.35% and for the liver, 1.08% for the kidneys, and 0.87% and for the spleen. The percentage differences in dose calculated for the two time-point protocol were -6.60% for the liver, 0.81% and for the kidneys, and -6.60% and for the spleen. For patient six it was found that compared to the four time-point protocol, the percentage differences in dose calculated for the three time point protocol were 3.17% for the liver and 6.85% for the kidneys. The percentage differences in dose calculated for the single time point protocol was 0% for the liver and 0% for the kidneys.

For both patients four and six the two time-point protocol dose calculation deviated less from the dose calculated in the four time point protocol when compared to the three time point protocol. The reason for this can be seen graphically through the TACs in the results section. The slope between the first and second date time point is shallower than the slope following the second time point. When the first time point is omitted, the fit model over estimates the dose as there is no shallower slope to factor in to the fit resulting in a higher TIAC and overall dose calculation. Omitting the first time point on day zero does not accurately capture the uptake period and therefore will overestimate the dose.

The second objective of this project is to analyze the percentage difference in dose to OAR determined by OLINDA and MIM. For patient four the calculated percentage difference between the values calculated between OLINDA and MIM ranged from 23.07% to 38.53%. This comparison shows agreement in dose between both softwares. As both softwares calculate dose differently and make different assumptions, the dose calculated is expected to vary slightly. For patient six the calculated percentage difference between the values calculated between OLINDA and MIM ranged from -3.65% to -21.11%.

8 Conclusion

The dosimetry protocol used by a clinic has to consider logistical factors as well as protocol accuracy. A four time-point protocol after each cycle of Lutathera provides the greatest amount of data to calculate the dose to organs at risk as well as lesions but is also the most laborious for dosimetrists and burdening towards patients. In order to be able to handle the workload for more patients as well as have patients agree to extra scans, three and single time point protocols also provide a viable option toward patient-specific dosimetry. In the case where patients do not wish to receive three extra SPECT/CT scans or clinic layout prohibits day zero imaging, two and three time point imaging protocols, respectively, can be used, however the single time point protocol offers less deviation from the four time-point protocol than the three time point protocol.

9 Limitations and Future Work

As stated earlier in this project, the three time-point protocol is being evaluated for the purpose of clinic logistics. OHSU cannot currently treat and image patients at the same location on day zero of treatment as the SPECT scanners have not produced research grade data and thus the most viable option for imaging would be the three time-point protocol. This clinic setup provides a limitation for the time being. The three time-point protocol was shown to consistently overestimate dose compared to the four time point protocol. This means that if dose modulation were to occur, a more conservative approach would be needed to increase the dose as the dose calculated is closer to the tissue limit. Since the three time point protocol is consistently overestimating dose, it may be important to reevaluate the SPECT capabilities on the hilltop campus where treatment occurs to begin using the four time point protocol.

In any case of protocol adoption, SPECT characterization needs to be performed on all SPECT units that will be used. This characterization will include determining corrections for geometric sensitivity, attenuation correction, scatter correction, uniformity, etc. This process is better outlined in the methods section as well as the literature.(24)(8)

An additional limitation of this project that will also be seen in future work is the difficulty in recruiting patients to return to the hospital for additional SPECT/CT scans. The longest protocols take eight days to complete which is often an insurmountable burden for the patients. Therefore, either the quickest protocol is adopted or the patient opts out of the study. Ideally, the single time point protocol will help to increase the sample size of a dosimetry study as well as reach the most amount of patients.

Future work could include dose modulation beyond halving and/or withholding treatment. The more that is known about the dose delivered to tumors and OARs, the more that can aid in a decision to modulate the dose by a deliberate amount to continue to minimize dose to OARs and maximize dose to tumors.

A second possibility for future work would be to use the distribution of the radiophar-

maceutical used in diagnosis of neuroendocrine tumors to provide bone marrow and lesion specific dosimetry. An excess of dose to the bone marrow can lead to myelosuppression which would lead a reduction in the injected activity. Better knowledge of bone marrow dose in addition to other OARs would be beneficial. The same is true for lesional dose. It is important to know the amount of dose received per unit of injected activity especially if injected activity is to be modulated.

With the conclusion of this project, the next steps would be to characterize the SPECT scanners that will be used, implement the chosen protocol, and begin to recruit patients. More patients that undergo scanning will add more statistical analysis capabilities to the work already done. More statistical analysis will allow dose modulation to begin with more information known.

References

[1] L. Geenen, J. Nonnekens, M. Konijnenberg, S. Baatout, M. D. Jong, and A. Aerts, "Overcoming nephrotoxicity in peptide receptor radionuclide therapy using [177lu]lu-dota-tate for the treatment of neuroendocrine tumours," *Nuclear Medicine and Biology*, vol. 102-103, pp. 1–11, 11 2021.

[2] G. Rindi, D. S. Klimstra, B. Abedi-Ardekani, S. L. Asa, F. T. Bosman, E. Brambilla, K. J. Busam, R. R. de Krijger, M. Dietel, A. K. El-Naggar, L. Fernandez-Cuesta, G. Klöppel, W. G. McCluggage, H. Moch, H. Ohgaki, E. A. Rakha, N. S. Reed, B. A. Rous, H. Sasano, A. Scarpa, J. Y. Scoazec, W. D. Travis, G. Tallini, J. Trouillas, J. H. van Krieken, and I. A. Cree, "A common classification framework for neuroendocrine neoplasms: an international agency for research on cancer (iarc) and world health organization (who) expert consensus proposal," *Modern Pathology*, vol. 31, 2018.

[3] E. Mora-Ramirez, L. Santoro, E. Cassol, J. C. Ocampo-Ramos, N. Clayton, G. Kayal, S. Chouaf, D. Trauchessec, J. P. Pouget, P. O. Kotzki, E. Deshayes, and M. Bardiès, "Comparison of commercial dosimetric software platforms in patients treated with 177lu-dotatate for peptide receptor radionuclide therapy," *Medical Physics*, vol. 47, 2020.

[4] L. Santoro, E. Mora-Ramirez, D. Trauchessec, S. Chouaf, P. Eustache, J. P. Pouget, P. O. Kotzki, M. Bardiès, and E. Deshayes, "Implementation of patient dosimetry in the clinical practice after targeted radiotherapy using [177lu-[dota0, tyr3]-octreotate," *EJNMMI Research*, vol. 8, 2018.

[5] E. Ilan, M. Sandström, C. Wassberg, A. Sundin, U. Garske-Román, B. Eriksson, D. Granberg, and M. Lubberink, "Dose response of pancreatic neuroendocrine tumors treated with peptide receptor radionuclide therapy using 177lu-dotatate," *Journal of Nuclear Medicine*, vol. 56, 2015.

[6] M. T. Madsen, Y. Menda, T. M. O'Dorisio, and M. S. O'Dorisio, "Technical note: Single time point dose estimate for exponential clearance," *Medical Physics*, vol. 45, 2018.

[7] H. Hänscheid, C. Lapa, A. K. Buck, M. Lassmann, and R. A. Werner, "Dose mapping after endoradiotherapy with 177 lu-dotatate/dotatoc by a single measurement after 4 days," *Journal of Nuclear Medicine*, vol. 59, 2018.

[8] M. Ljungberg, A. Celler, M. W. Konijnenberg, K. F. Eckerman, Y. K. Dewaraja, and K. Sjögreen-Gleisner, "Mird pamphlet no. 26: Joint eanm/mird guidelines for quantitative 177lu spect applied for dosimetry of radiopharmaceutical therapy," *Journal of Nuclear Medicine*, vol. 57, 2016.

[9] E. Hippeläinen, M. Tenhunen, H. Mäenpää, and A. Sohlberg, "Quantitative accuracy of 177lu spect reconstruction using different compensation methods: phantom and patient studies," *EJNMMI Research*, vol. 6, 2016.

[10] Y. K. Dewaraja and B. J. Van, "(2021)lu-177 dotatate anonymized patient datasets: Lesion and organ volumes of interest [data set], university of michigan - deep blue data. https://doi.org/10.7302/vhrh-qg23," 2021.

[11] X. Hou, J. Brosch, C. Uribe, A. Desy, G. Böning, J. M. Beauregard, A. Celler, and A. Rahmim, "Feasibility of single-time-point dosimetry for radiopharmaceutical therapies," *Journal of Nuclear Medicine*, vol. 62, 2021.

[12] B. N. Lab, "Nuclear science data center,"

[13] E. J. Hall and A. J. Giaccia, *Radiobiology for the radiologist: Seventh edition.* 2012.

[14] A. Dash, M. Pillai, and K. F. Jr, "Production of (177)lu for targeted radionuclide therapy: Available options," *Nucl Med Mol Imaging*, 2017.

[15] S. Cherry, J. Sorenson, and M. Phelps, "Physics in nuclear medicine," *Physics in Nuclear Medicine*, 2012.

[16] S. M. Bentzen, L. S. Constine, J. O. Deasy, A. Eisbruch, A. Jackson, L. B. Marks, R. K. T. Haken, and E. D. Yorke, "Quantitative analyses of normal tissue effects in the clinic (quantec): An introduction to the scientific issues," *International Journal of Radiation Oncology Biology Physics*, vol. 76, 2010.

[17] W. E. Bolch, K. F. Eckerman, G. Sgouros, S. R. Thomas, A. B. Brill, D. R. Fisher, R. W. Howell, R. Meredith, and B. W. Wessels, "Mird pamphlet no. 21: A generalized schema for radiopharmaceutical dosimetry-standardization of nomenclature," *Journal of Nuclear Medicine*, vol. 50, 2009.

[18] "The 2007 recommendations of the international commission on radiological protection. icrp publication 103.," *Annals of the ICRP*, vol. 37, 2007.

[19] P. A. Feller, V. J. Sodd, and J. G. Kereiakes, "Using the s tables of mird pamphlet 11.," *Journal of Nuclear Medicine*, vol. 18, 1977.

[20] J. F. Fowler, "21 years of biologically effective dose," *British Journal of Radiology*, vol. 83, 2010.

[21] R. G. Dale and B. Jones, "The assessment of rbe effects using the concept of biologically effective dose," *International Journal of Radiation Oncology Biology Physics*, vol. 43, 1999.

[22] S. K. Gupta, S. Singla, P. Thakral, and C. S. Bal, "Dosimetric analyses of kidneys, liver, spleen, pituitary gland, and neuroendocrine tumors of patients treated with 177lu-dotatate," *Clinical Nuclear Medicine*, vol. 38, 2013.

[23] M. Sandström, U. Garske, D. Granberg, A. Sundin, and H. Lundqvist, "Individualized dosimetry in patients undergoing therapy with 177lu-dota-d-phe1-tyr3-octreotate," *European Journal of Nuclear Medicine and Molecular Imaging*, vol. 37, 2010.

[24] J. Beauregard, M. Hofman, J. Pereira, P. Eu, and R. Hicks, "Quantitative (177)lu spect (qspect) imaging using a commercially available spect/ct system," *Cancer Imaging*, 2018.

[25] P. M. Kasi, C. L. Maige, F. Shahjehan, J. M. Rodgers, D. L. Aloszka, A. Ritter, M. L. Andrus, J. M. Mcmillan, K. Mody, A. Sharma, and M. K. Jain, "A care process model to deliver177lu-dotatate peptide receptor radionuclide therapy for patients with neuroendocrine tumors," *Frontiers in Oncology*, vol. 9, 2019.

We acknowledge Yuni Dewaraja at the University of Michigan for providing access to Lu-177 patient imaging data and segmentations obtained with support from R01EB022075 awarded by NIBIB and R01CA240706 awarded by NCI, NIH. Data were shared via the University of Michigan Deep Blue Data sharing repository.